NASA CONTRACTOR REPORT

NASA CR-704

NASA CR-704

GPO PRICE $ _____

CFSTI PRICE(S) $ _____

Hard copy (HC) 3.00

Microfiche (MF) 1.30

ff 653 July 65

[redacted]

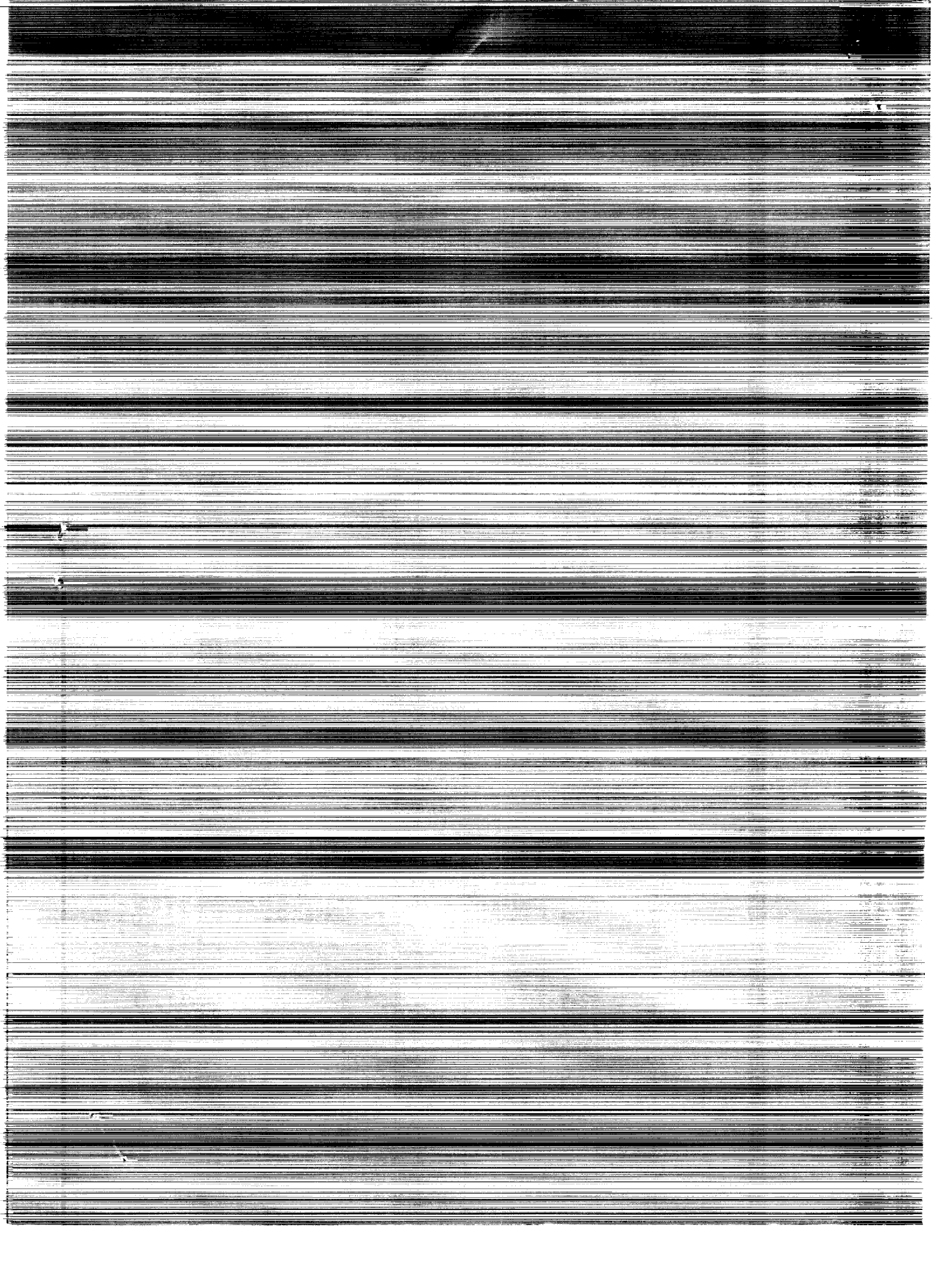

NASA CR-704

THEORY OF ELECTROSTATIC PLANAR AND SPHERICAL PROBES

By Lee W. Parker

Prepared under Contract No. NAS 5-9088 by
MT. AUBURN RESEARCH ASSOCIATES, INC.
Cambridge, Mass.

for Goddard Space Flight Center

NATIONAL AERONAUTICS AND SPACE ADMINISTRATION

For sale by the Clearinghouse for Federal Scientific and Technical Information
Springfield, Virginia 22151 – Price $2.50

ABSTRACT

In the theory of an electrostatic plasma probe, the current is calculated by considering all possible trajectories corresponding to particles which impinge on the probe surface. The trajectories may or may not be populated, depending on the geometry of the probe and the structure of the potential distribution in its vicinity, as well as on the particle velocity distribution at infinity. By considering which trajectories are populated and which are not, a theoretical expression is obtained for the current collected by a planar probe assumed to be embedded in the skin of a large satellite in the ionosphere plasma. This expression is in the form of an integral over velocity space. The analytical properties of the domain in velocity space which corresponds to populated trajectories are investigated. The shape of the domain governs the current characteristics of the probe. General formulae are derived which depend on the shape of the domain. An approximate theory is employed to obtain an analytical form for the shape of the domain, and expressions are derived for the current characteristics of the probe. Comparison is made between the theoretically derived characteristics and those computed by numerical trajectory calculations. An approximate theory is also employed for the spherical probe, based on a power-law potential model. The planar and spherical probes are compared. The circumstances under which Druyvesteyn relations exist are investigated for the planar and spherical probes. Under the assumption of a spherically symmetric potential, formulae are derived for the current collected by a spherical probe moving through a plasma. The theoretical current collection based on the power-law potential model is compared with the current based on the sheath model.

TABLE OF CONTENTS

THEORY OF A STATIONARY PLANAR PROBE

I. INTRODUCTION

Measurements of the density and temperature of charged particles in the ionosphere have recently been made using a circular planar probe, flush-mounted in the skin of the carrier satellite.[1] The probe essentially consists of a grid maintained at an arbitrary potential with respect to the satellite. There may also be inner grids or collecting electrodes. The current entering the outer grid or aperture of the probe, plotted as a function of the grid potential, is called the current characteristic. It is possible, by suitable interpretation of the plot, to infer certain parameters (moments) associated with the charged particle velocity distributions in the undisturbed plasma "at infinity." The task of interpretation involves separating out the specific geometric-electric effects of the probe which perturbs the plasma.

In the case of a retarding probe, whose outer grid is biased so as to repel the particles of a given sign, the current characteristic is frequently free of geometric effects, so that it may be interpreted rather directly in terms of the velocity distribution at infinity. For example, under certain circumstances, it is possible to obtain the velocity distribution directly from the second derivative of the current characteristic with respect to the retarding potential. This technique is usually associated with the name of Druyvesteyn[2], who applied it to his measurements, although this relationship had been recognized earlier by Mott-Smith and Langmuir[3] (Reference 3, p. 753). Because of its specific association, the relation between the second derivative of the current and the velocity distribution function will be referred to here as a "Druyvesteyn relation."

In the case of an accelerating probe, the outer grid is biased so as to attract the particles of a given sign. The current characteristic will be referred to as the "probe current characteristic." This characteristic usually cannot be interpreted so directly as the retarding probe characteristic because the effects of geometry and of the velocity

distribution are strongly coupled in the resulting current. However, an important modification may be made in which the potential of the outer grid is held fixed while a variable bias is applied to an inner collecting electrode (see Fig. 1) so as to repel particles which have passed through the outer grid. The curve obtained when the current entering the collecting electrode is plotted as a function of the retarding potential on the collector will be referred to as the "retarded current characteristic" (not to be confused with the characteristic of a retarding probe). A Druyvesteyn relation may exist for this characteristic under certain circumstances, which are discussed in this paper.

When the ambient plasma is collision-free, the details of the particle trajectories will determine the effects of geometry on the current-collecting characteristics of the accelerating probe. In particular, a significant role will be played by trajectories which intersect the surface of the satellite. This paper will be primarily concerned with the effects of trajectory intersections. The term "intersection" will be taken here to refer to a particle trajectory which intersects the surface of the satellite, not only at the probe surface (grid) but also at some other point on the satellite. This can occur whether or not the trajectory can connect with infinity according to energy conservation. Since the trajectories are dynamically reversible for the time-independent problem, a trajectory can be analyzed by following it backwards in time to its origin. Starting from the probe surface, a particle which has the energy to escape to infinity may instead strike the satellite surface, i.e., its trajectory may intersect the satellite surface. If there is no reflection or photoelectric emission, the trajectory is not occupied. Therefore, it contributes nothing to the current and will said to be "excluded." If the particle has the energy to escape to infinity and does not strike the satellite, however, its trajectory is an occupied one and does contribute to the current. Whether an intersection does or does not occur will depend

on the angle θ made by the initial velocity vector (at the probe surface) with the outward normal to the probe surface. Assuming the particle has the energy to escape to infinity, it will (generally) do so when $\theta = 0$, i.e., when the initial velocity is vertical. When $\theta = \pi/2$, the trajectory is a grazing one and the particle certainly intersects the surface. There is, therefore, a critical value of the angle, for greater values of which the trajectories are excluded or unoccupied because of intersections. The exclusion of trajectories at angles θ less than $\pi/2$ results in a modification of the current characteristics similar to the effect of the finite sheath in the theory of Mott-Smith and Langmuir[3]. (Formulae which correspond to the infinite sheath limit in the Mott-Smith-Langmuir theory will be called "Langmuir formulae.") Moreover, a Druyvesteyn relation may not exist when exclusion effects are important. Modifications of the theory of spherical probes due to exclusion effects are discussed by Hall[4], Bernstein and Rabinowitz[5], and Al'pert, Gurevich and Pitaevskii[6].

When the distribution of particle velocities at infinity is not isotropic, e.g., a streaming Maxwellian, it is not possible to express the current to a planar probe in a simple analytic form. However, when the distribution of velocities is isotropic, the current may be expressed in a form which exhibits clearly the effect of trajectory exclusions. It is possible in only one case to express the probe current analytically when the velocity distribution is arbitrary. This is the case of a spherical probe in a spherically symmetric potential. The current depends only on the distribution in speeds at infinity. Because of its general interest a discussion of this case is included here.

In the next section, assuming a simplified geometry, the theory of the particle current density at the outer grid of an accelerating planar probe is treated, assuming a Maxwellian distribution of particle velocities at infinity, and absorption of particles at the surface. Intersections are discussed in terms of a curve in "trajectory space,"

representing the demarcation between the domains of occupied and unoccupied or excluded trajectories. Expressions are presented for the probe current and the retarded current characteristics in terms of an undetermined algebraic function representing the boundary of the excluded portion of trajectory space. The one-dimensional and three-dimensional limiting cases are discussed.

In Section III, current characteristics obtained by numerical trajectory calculations[7] are presented for the unshielded electric field of the OGO probe[8]. A numerically-determined boundary curve in trajectory space is discussed.

In Section IV, an approximate theory is employed to obtain an analytic expression for the boundary curve in trajectory space. The current characteristics based on this analytic expression are derived and a comparison is made with the results of the trajectory computations of Section III. The limiting cases are discussed.

Appendix A treats the effects of intersections on the current to a sphere, assuming a spherically symmetric potential described by a power law. An approximate analytic expression is derived for the boundary curve in trajectory space. The resulting current characteristics are derived, with the exponent as a parameter, and compared with the Langmuir formulae.

In Appendix B, the current characteristics are derived for a general isotropic distribution. A Druyvesteyn relation is shown to exist, under reasonable assumptions, for the retarding probe characteristic and for the retarded current characteristic of the accelerating probe, regardless of intersections. The accelerating probe current characteristic is shown to have the classical linear form in the absence of intersection effects.

In Appendix C, the characteristics of accelerating probes are derived for general isotropic distributions. The approximate one-parameter theories of Appendix A and Section IV are applied to the

cases of the spherical probe and the planar probe, respectively. In the presence of intersection effects, the characteristics are linear only for large values of probe potential, and have slopes less than those of the classical Langmuir formulae. A relation similar to the Druyvesteyn relation is found for the sphere.

In Appendix D, the exceptional case of a spherical probe in a spherically symmetric potential is discussed. The velocity distribution is assumed rotationally symmetric but otherwise arbitrary. The current to the probe is obtained by integration over the probe surface, taking into account the effects of trajectory intersections when the potential is a prescribed power law. A Druyvesteyn relation is shown to hold for an arbitrary speed distribution at infinity. The expression obtained for the power-law model when the velocity distribution is a Maxwellian with drift is compared to that obtained on the basis of a sheath model.

II. THE THEORY OF THE PROBE CHARACTERISTICS

The current of particles passing through unit area at any point $\vec{r}$ in ordinary space, i.e., the vector current density, may be represented as a triple integral over velocity space of the form

$$\vec{J}(\vec{r}) = \iiint f(\vec{r}, \vec{v})\, \vec{v}\, d^3\vec{v} \tag{1}$$

where $\vec{v}$ is the vector velocity of a particle passing through the point $\vec{r}$. The function $f(\vec{r}, \vec{v})$ is the density of points in six-dimensional phase space. In the time-independent collision-free case the function f is given by the solution of the Boltzmann equation:

$$\vec{v} \cdot \nabla_r f + \vec{a} \cdot \nabla_v f = 0 \tag{2}$$

where $\vec{a}$ is the vector acceleration of the particle, and the gradient operators ∇_r and ∇_v represent differentiations with respect to the components of $\vec{r}$ and $\vec{v}$, respectively. The function f will be referred to as the "distribution function".

A planar probe embedded in the skin of a large satellite[8] (large compared with dimensions such as probe radius and Debye length) may be approximately represented by the geometry shown in Fig. 1, in which the satellite skin is considered to extend to infinity in the form of a flat plane. The satellite skin will be assumed to be at the potential of the ambient plasma. Since the probe potentials of interest will be considerably larger than the difference of potential between the satellite and the plasma, the results following from this assumption should not be greatly in error. The normal component of current density at a point $\vec{r}_p$ on the outer grid of the probe shown in Fig. 1 is given by the scalar triple integral over velocity space:

$$j(\vec{r}_p) = \iiint f(\vec{r}_p, \vec{v})\, v_z\, d^3\vec{v}$$

where v_z is the normal component of velocity of a particle passing through the point $\vec{r}_p$.

When the forces have the property that the total energy is constant along any particle trajectory, then the function f is constant along that particle trajectory. Thus, if the distribution function f is known on a given boundary C in phase space, then at any point $\vec{r}$ along a trajectory which connects with C we have

$$f(\vec{r},\vec{v}) = f_c(\vec{r}_c,\vec{v}_c) \tag{4}$$

where

$$v^2 + \frac{2}{m}\Phi(\vec{r}) = v_c^2 + \frac{2}{m}\Phi(\vec{r}_c) = \frac{2}{m}E \tag{5}$$

A boundary of this type is illustrated in a two-dimensional representation of phase space in Fig. 2. In Eqs. (4) and (5), m is the particle mass, Φ is the scalar potential energy function, E is the (constant) total energy, and the subscript C refers to points on the boundary C.

For the probe geometry depicted in Fig. 1, the boundary C is comprised of two parts, A and B, where A refers to the entire satellite surface and B represents all other points at infinity above the plane. On the two boundaries, A and B, the corresponding distribution functions f_A and f_B will be assumed known. On the boundary at infinity (B) the distribution function may be assumed, for many physical situations of interest, to be given by the Maxwellian function

$$f_B(\vec{r}_B,\vec{v}_B) = \frac{1}{\pi^{3/2}} e^{-(\vec{v}_B - \vec{v}_s)^2} \tag{6}$$

where f_B is dimensionless and is defined in units of the ambient particle density denoted by n_o. The dimensionless velocities $\vec{v}_B$ and $\vec{v}_s$ are

defined in units of the thermal velocity $(2kT/m)^{\frac{1}{2}}$, T being the temperature. The velocity vector $\vec{v}_s$ is defined here as the vector Mach number and represents the dimensionless mean velocity of the gas of particles with respect to the satellite.

If ϕ denotes the dimensionless potential energy defined in units of the thermal energy kT, then, according to Eqs. (4) and (5), the distribution function at $\vec{r}_p$ for trajectories which connect with infinity (B) is given by

$$f(\vec{r}_p, \vec{v}) = \frac{1}{\pi^{3/2}} \exp\left[-v_B^2 - v_s^2 + 2\vec{v}_B \cdot \vec{v}_s\right] \quad (7)$$

where

$$v_B^2 = v^2 + \phi(\vec{r}_p) \quad (8)$$

and ϕ is assumed to vanish at infinity.

On the satellite surface, boundary A, the distribution function is that which describes the emission of particles from the surface, e.g., photoelectrons, secondary electrons, or reflected particles. If there is no emission of any kind, the distribution function f vanishes at the surface. It will be assumed in this paper that all charged particles incident on the surface are neutralized and that none are emitted so that f_A is zero. Thus, f is zero for trajectories which intersect the satellite surface. It will also be assumed that the probe potential (ϕ) is negative and that there are no particles occupying trapped trajectories. The Mach vector $\vec{v}_s$ will be assumed normal to the probe, defining a z-axis whose positive direction is upward as in Fig. 1. The normal component of the current density (j) will be considered at the center of the probe for simplicity, since the geometry of the integrals is then rotationally symmetric. For off-center points, the integrals are more complicated but the essential ideas would be the same.

A. THE ACCELERATING PROBE CURRENT CHARACTERISTIC

It will be convenient to employ cylindrical coordinates for the velocity space, with the v_z-axis of the system along the direction of $\vec{v}_s$. Thus, v_z and v_r will represent the axial and radial components of the dimensionless velocity, respectively. With the use of Eqs. (3), (7), and (8), the current density at the center of the probe can be written as the ratio

$$\frac{j}{j_o} = 4e^{-\phi - v_s^2}\int_0^\infty e^{-v_z^2} v_z \, dv_z \int_{v_m(v_z)}^\infty e^{-v_r^2 + 2v_s v_{z_\infty}} v_r \, dv_r \quad (9)$$

where j_o is the ambient thermal current density defined by

$$j_o \equiv n_o \left(\frac{kT}{2\pi m}\right)^{1/2} \left[e^{-v_s^2} + \sqrt{\pi}\, v_s (1 + \mathrm{erf}\, v_s) \right] \quad (10)$$

In Eq. (9), ϕ is the potential energy of a particle at the probe surface, and v_{z_∞} is the value of v_z at infinity, which depends on the local values of v_z and v_r through the trajectory. The lower limit $v_m(v_z)$ of the v_r-integral is, in general, an unknown function of v_z representing the boundary of the domain, in v_r-v_z space, in which the integrand is non-vanishing. This is the domain in which trajectories are not only energetically possible but also connect with infinity, i.e., they do not intersect the surface of the satellite. An example of such a boundary is shown in Fig. 3, where the shaded domain represents trajectories which are unoccupied, either because they are not energetically possible or because they intersect with the satellite surface. Thus, recalling that the trajectories are to be followed backwards in time, we see that the integration in Eq. (9) extends over the domain above and to the right of some curve $v_r = v_m(v_z)$ in Fig. 3. For negative values of v_z, the trajectories are unoccupied since they clearly come from the satellite surface, which has been assumed non-emitting. For

positive values of v_z, it is not simple to distinguish between those trajectories which are unoccupied because they are energetically impossible and those which are unoccupied because they originate at the satellite surface. Thus, for positive values of v_z, the curve $v_m(v_z)$ must in general be determined by detailed trajectory calculations in a given electric field. Also, for an arbitrary electric field, the connection between v_{z_∞} and v_r and v_z cannot be determined analytically, and hence, the evaluation of the integrand in Eq. (9), even for the allowed domain, must be performed numerically. However, for the case of zero Mach number ($v_s = 0$), it is possible to gain considerable analytic insight, and it is with this case that we will henceforth be concerned.

For $v_s = 0$, the integrand and differentials in Eq. (9) may be expressed in terms of v_z^2 and v_r^2, and it is therefore convenient to represent the allowed domain of integration as in Fig. 4. If there were no intersections, the allowed domain in Fig. 4 would be the entire quadrant except for the triangular area representing points such that $v_r^2 + v_z^2 < V_o$, where V_o denotes the positive value $-\phi$, i.e., the magnitude of the probe potential. The forbidden triangle represents points which cannot connect energetically with infinity. (See also Reference 3, pp. 755-6.) However, the effect of intersections is to exclude also a neighborhood of the entire v_r^2 - axis (near $v_z = 0$) from the allowed domain. This is due to the fact that points on this axis correspond to grazing trajectories, and that grazing particles will be deflected into the probe surface by any attractive field, however weak. This situation is peculiar to the planar probe, and does not apply to the case of a sphere, in which case only a finite portion of the v_r^2 - axis may be excluded. (See Appendix A for the special case of the sphere.)[9] The closer a trajectory is to grazing incidence, i.e., the closer to the v_r^2 - axis its representative point lies, the larger is the required value of v_r^2 to correspond to an allowed trajectory. Thus, rather than the v_r^2 - axis, i.e., curve (c) in Fig. 4, the boundary of

the allowed domain may be some curve such as (a). This boundary may possibly intersect the line $v_r^2 + v_z^2 = V_o$ in Fig. 4, in which case the allowed domain would be above and to the right of both curves. If intersections are not very important, the curve (a) moves to the left, i.e., toward the axis (curve (c)). If intersections are very important, the boundary curve may be like (b) in Fig. 4. As intersections become dominant, the boundary curve may move to the right and tend toward the vertical line (d). All boundary curves probably pass through the point $v_z^2 = V_o$ on the v_z^2 - axis. That is, unless the electric field is very peculiar, the trajectory should be capable of connecting with infinity regardless of intersections provided only that v_z^2 exceeds V_o. An important distinction exists between points to the right of and points to the left of the vertical line (d), i.e., $v_z^2 = V_o$ in Fig. 4. For points to the left of (d), an interchange occurs between the kinetic energies associated with radial and axial components of velocity. That is, some axial kinetic energy must be transformed into radial kinetic energy as a particle comes in from infinity and arrives at the attracting probe surface. For example, a particle may arrive without any axial velocity, all of its kinetic energy having gone into radial motion. However, for points to the right of (d), an interchange may or may not occur between the kinetic energies associated with radial and axial motions. These motions may be considered as independent, as far as the current integral (see Eq. (11) below) is concerned, and the consequence is that in certain cases contributions to the right of (d) reflect directly the velocity distribution at infinity, independently of the geometry of the probe. It is shown in Appendix B that this property applies to an isotropic distribution at infinity, which may otherwise be arbitrary.

In the following analysis it will be assumed that the intersection-governed part of the boundary curve in the velocity space is represented by a curve such as (a) in Fig. 4. This behavior is suggested by the results of numerical calculations. (See Section III.)[7]

If $v_s = 0$, then Eq. (9) may be expressed in the form

$$\frac{j}{j_o} = e^{V_o} \int_0^\infty e^{-z - \chi_m(z)} \, dz \tag{11}$$

where j_o denotes the thermal ambient current density $n_o(kT/2\pi m)^{\frac{1}{2}}$. (See Eq. (10)). In Eq. (11), z represents v_z^2, x represents v_r^2, V_o represents the positive value $-\phi$, i.e., the magnitude of the attractive probe potential energy, and $x_m(z)$ represents the boundary in x-z space between the occupied and unoccupied domains. The x-z space will be referred to as the "trajectory space." (Confusion should not result from the use of this notation, since no reference is made to spatial coordinates.) The boundary curve is assumed to be given for the present case as in Fig. 5, where it consists of three regions:

$$\text{(I)} \quad x_m(z) = 0 \quad (z > V_o) \tag{12a}$$

$$\text{(II)} \quad x_m(z) = V_o - z \quad (z_1 \leq z \leq V_o) \tag{12b}$$

$$\text{(III)} \quad x_m(z) > V_o - z \quad (0 \leq z < z_1) \tag{12c}$$

In Region III, the form of $x_m(z)$ is due to intersections and is not expressible analytically in general. Regions II and I represent the purely energetic requirement on the trajectories, namely, the relationship

$$x + z - V_o \geq 0 \tag{13}$$

Then $x_m(z)$ is given by $V_o - z$ or zero, whichever is greater.

On the basis of the assumed behavior of the boundary curve in trajectory space as shown in Fig. 5, Eq. (11) yields the resulting current density:

$$\frac{j}{j_o} = g_1 + g_2 + g_3 \tag{14}$$

where

$$g_1 = e^{V_o} \int_{V_o}^{\infty} e^{-z}\, dz = 1 \tag{15}$$

$$g_2 = e^{V_o} \int_{z_1}^{V_o} e^{-z-(V_o-z)}\, dz = V_o - z_1 \tag{16}$$

$$g_3 = e^{V_o} \int_{0}^{z_1} e^{-z-\chi_m(z)}\, dz \tag{17}$$

Now, in the case of no intersections, z_1 vanishes, and the current density becomes

$$\frac{j}{j_o} = g_1 + g_2 = 1 + V_o \tag{18}$$

which is the classical Langmuir formula.[3] However, when intersections are present, z_1 does not vanish and the current is less than that given by Eq. (18) since g_3 is always less than z_1. (See Section IV.)

It is of interest to compare the current density derived here with the current density of attracted particles which would enter the surface of a charged sphere at rest in a plasma. The current density entering the sphere would be given by Eq. (18), provided that the potential is spherically symmetric and falls off less rapidly than the inverse square of the radial distance. If the potential is spherically symmetric and falls off like the inverse n-th power of the distance, where the exponent n exceeds 2, then, as is shown by an approximate analytical calculation given in Appendix A, the current density rises less rapidly with V_o than is indicated by Eq. (18). In the limit of large values of the exponent n, the ratio j/j_o approaches unity for all values of V_o. In this limit the one-dimensional case of constant current is approached. Similar conclusions are arrived at in Reference 6 (p. 230).

The two terms in the formula $1 + V_o$ of Eq. (18) represent distinctly different types of trajectory contributions. Due to the special mathematical form of the integral in this symmetric problem, the term represented by unity may be considered as arising from the contributions of trajectories in which only the z-component of velocity is altered in coming from infinity to the probe. It reflects directly the integral over the distribution of the speeds at infinity. This is generally true for isotropic velocity distributions at infinity, as is shown in Appendix B. Thus, it has essentially a one-dimensional character, and is probably independent of the effects of intersections, i.e., of the geometry of the probe. However, the term represented by V_o arises from trajectory contributions in which there has been an interchange of energy between the radial and axial components of velocity. It is associated with geometric "convergence" or confluence of particle streams, and reflects the geometric influence of the probe. This term is likely to be affected by intersections in that its magnitude would be reduced. It tends to vanish in the limit in which intersections are so dominant that the problem becomes essentially one-dimensional (e.g., a very thin sheath).

B. THE RETARDED CURRENT CHARACTERISTIC

If a collecting electrode is placed close to and behind the probe grid shown in Fig. 1, and the collecting electrode is biased so as to repel particles coming through the grid, a retarded current characteristic may be obtained. Let the retarding potential energy of the collecting electrode with respect to the outer grid be denoted by V in units of kT, where V is positive. Then the current collected is less than that entering the grid due to the fact that some of the attracted particles incident at the grid cannot overcome the potential barrier V. The problem is one-dimensional in that only the kinetic energy associated with the z-component of velocity is affected. Holding the outer grid potential fixed at V_o, the current collected across the potential barrier V is given by the following modification of Eq. (11):

$$\frac{j'}{j_o} = e^{V_o} \int_V^\infty e^{-z - \chi_m(z)} \, dz \tag{19}$$

A consequence of the form of Eq. (19) is that the function $x_m(z)$ may be inferred from an experimental measurement of j'/j_o as a function of V. Taking the derivative of both sides with respect to V, we have

$$\chi_m(V) = V_o - V - \ln\left[-\frac{d}{dV}\left(\frac{j'}{j_o}\right)\right] \tag{20}$$

This formula will be referred to in the discussion of Section III.

Assuming $x_m(z)$ has the form given by Eqs. (12), Eq. (19) may be expressed according to three possible cases:

(a) $0 \le V < z_1 < V_o$

$$\frac{j'}{j_o} = e^{V_o} \int_V^{z_1} e^{-z - \chi_m(z)} \, dz \quad + 1 + V_o - z_1 \tag{21}$$

(b) $z_1 \leq V \leq V_o$

$$\frac{j'}{j_o} = V_o - V + 1 \tag{22}$$

(c) $V > V_o$

$$\frac{j'}{j_o} = e^{V_o - V} \tag{23}$$

In Eq. (21), $x_m(z)$ is the unknown function determined, say, by trajectory intersections. Thus, the characteristic is linear in a portion of the range of V below V_o, and exponential for V above V_o, with continuity of value and slope at $V = V_o$. For small values of V, the characteristic is truncated due to exclusion of trajectories by intersections with the satellite surface. This behavior is illustrated by curves in Fig 6, which are derived in Section IV on the basis of an approximate theory of intersections. The form of Eq. (23) suggests that a Druyvesteyn relation may hold for the retarded current characteristic of the accelerating probe. This question is explored in Appendix B.

III. NUMERICAL CALCULATIONS

For the planar probe geometry[8] shown in Fig. 1, detailed numerical trajectory calculations have been performed[7] which yield insight into the effect of trajectory intersections on the current and on the shape of the allowed domain in velocity space. The problem may be approximated by one in which an infinite plane is maintained at zero potential, except for a circular area representing the probe, which is maintained at a different potential. The potential distribution in the absence of space charge (Laplace solution) is represented by the contour plot in Fig. 7. The function depicted in Fig. 7 corresponds to unit potential on the probe. The potential everywhere is scaled by the factor V_o when the probe potential is V_o.

The current ratio j/j_o was calculated as a function of V_o (see Eqs. (10) and (11) for definitions). This characteristic is shown for V_o in the range (0, 16) in Fig. 8 and in the range (0, 100) in Fig. 9. The numerical points are designated by circles. For large values of V_o the characteristic is a straight line to within the accuracy of the calculation. The slope is less than unity, due to trajectory exclusions. Also plotted in Fig. 8 and 9 are analytical curves derived in Section IV. Further detailed numerical calculations were performed for a grid potential of $V_o = 45.54$, corresponding to 5.1 volts for an ambient temperature of 1300°K. The derivative $d(j/j_o)/dz$ was computed as a function of z, where z has been defined previously in Section II as the kinetic energy, in units of kT, associated with the normal component of velocity at the probe surface. This computed derivative is shown in Fig. 10. There is a flat plateau just below $z = 45.54$, and a sharp transition at $z = 45.54$ to an exponential. The falling-off for z near zero is clearly a manifestation due to trajectory intersections. The boundary for the domain of allowed trajectories in the trajectory space, i.e., the function $x_m(z)$ in Eq. (11) or Eq. (19), may be obtained from the function in Fig. 10 by the use of Eq. (20), in which V is replaced by z and $-dj'/dV$ is replaced by dj/dz. The resulting graph for $x_m(z)$ is shown in Fig. 11.

The computed domain in Fig. 11 of allowed trajectories in trajectory space suggests that Fig. 5 is a good representation. That is, intersections affect the domain for z between 0 and 45.54, i.e., where geometrical effects are important. The current j/j_o, for $V_o = 45.54$, is given by the area under the curve in Fig. 10. This is approximately 35, consistent with Fig. 9.

The retarded current characteristic may be obtained from the numerical data by integrating the curve in Fig. 10 ($d(j/j_o)/dz$) from V to infinity, where V is the repulsive potential barrier which particles must overcome in going from the outer grid to the collector. The resulting characteristic corresponds nearly exactly to the theoretical curve with b = 1 in Fig. 6. A discrepancy occurs in the vicinity of V = 11, where the numerical calculations (dotted line) show a less abrupt transition from the flat portion to the linear portion of the characteristic.

IV. APPROXIMATE THEORY OF INTERSECTIONS

By the use of an impulse approximation, it is possible to derive a theoretical expression for the boundary curve $x_m(z)$ of the allowed domain in trajectory space (see Figs. 5 and 11). This may then be used to obtain analytic expressions for the current characteristics such as given by Figs. 6 and 8.

Let the velocities be taken in units of $(2kT/m)^{\frac{1}{2}}$ and the energies in units of kT. Then the equation for the finite change in the normal component of velocity (Δv_z) due to the normal component of the potential energy gradient ($\partial \Phi / \partial z$) may be written:

$$\Delta v_z = -\frac{1}{2} \int_0^\infty \frac{\partial \phi}{\partial z} \frac{ds}{v} \tag{24}$$

Equation (24) equates the momentum change to the impulse of the force, as one follows the particle backwards in time from the center of the probe, where s = 0, to either infinity or the satellite surface. v is the instantaneous speed of the particle and ds/v represents the differential of time. (In the integrand of Eq. (24), z clearly denotes the spatial coordinate z rather than v_z^2 as in the previous sections.)

The integral in Eq. (24) may be written

$$\Delta v_z = -\frac{1}{2} \left\langle \frac{1}{v} \right\rangle \int_0^\infty \frac{\partial \phi}{\partial z} ds \tag{25}$$

if by $\langle 1/v \rangle$ we mean an average value of $1/v$ over the trajectory. We propose to approximate the integral of Eq. (25) by replacing $\langle 1/v \rangle$ by b/v, where v is the speed of the particle at s = 0, i.e., the

center of the probe grid (see Fig. 1), and b is an average constant or "fudge factor" which is difficult to evaluate. Since, on following the particle backwards in time from the attracting probe, v generally decreases with s, b is probably numerically greater than unity. If b varies sufficiently slowly, this approximation should not be greatly in error. The proposed approximation is equivalent to assuming that all trajectories are straight lines or rays radiating from the center of the probe to infinity. The approximation should become accurate when the critical trajectories are nearly grazing ones.

Since the integral in Eq. (25) must be equal to the probe potential, V_o, Eq. (25) may be approximated by

$$\Delta v_z \simeq -\frac{b}{2}\frac{V_o}{v} \tag{26}$$

where b is a constant of the order of and greater than unity. The velocities v and v_z are the initial values at the probe center. Thus, intersections will occur if

$$v_z < -\Delta v_z \simeq \frac{b}{2}\frac{V_o}{v} \tag{27}$$

or, on squaring both sides and rearranging, if

$$x < x_m(z) = \frac{b^2 V_o^2}{4z} - z \tag{28}$$

In Eq. (28), z denotes v_z^2 and x denotes v_r^2, as defined in Section II.

Equation (28) will be used as an analytic boundary curve in trajectory space. The theoretical allowed domain based on Eq. (28) is plotted in Fig. 11, assuming b = 1 and V_o = 45.54, for comparison with the points obtained by numerical trajectory calculations. The analytic intersection curve deviates considerably from the numerically determined points for values of $z < z_1 = 11.385 = (45.54)/4$. However, the analytic and numerical curves intersect the line 45.54-z at very nearly the same value of z. This point will be discussed further below.

Using $x_m(z)$ as given by Eq. (28) in Eq. (12c), and with z_1 given by $b^2V_o/4$, Eqs. (15)-(17) become:

$$g_1 = 1 \tag{29}$$

$$g_2 = (1 - b^2/4)V_o \tag{30}$$

$$g_3 = e^{V_o}\int_0^{\frac{b^2}{4}V_o} e^{-\frac{b^2V_o^2}{4z}}\,dz = \frac{b^2V_o^2}{4}e^{V_o}\int_{V_o}^{\infty}\frac{e^{-y}}{y^2}\,dy$$

$$= \frac{b^2}{4}V_o - \frac{b^2}{4}V_o^2 e^{V_o}E_1(V_o) \tag{31}$$

where $E_1(p)$ denotes the exponential integral

$$E_1(p) \equiv \int_p^{\infty}\frac{e^{-t}}{t}\,dt \tag{32}$$

Thus, Eq. (14) gives the normalized current density as the sum of Eqs. (29)-(31):

$$\frac{j}{j_o} = 1 + V_o - \frac{b^2}{4} V_o^2 e^{V_o} E_1(V_o) \qquad (33)$$

For small V_o, $E_1(V_o)$ increases like ln $(1/V_o)$ and $V_o^2 E_1(V_o)$ is dominated by V_o, so that

$$\frac{j}{j_o} \simeq 1 + V_o \quad \text{for} \quad V_o << 1 \qquad (34)$$

For large V_o, $E_1(V_o)$ decreases like e^{-V_o}/V_o, so that

$$\frac{j}{j_o} \sim \left(1 + \frac{b^2}{4} - \frac{b^2}{2V_o} + \cdots\right) + \left(1 - \frac{b^2}{4}\right) V_o \qquad (35)$$

for $V_o >> 1$

Equation (33) is plotted in Figs. 8 and 9, for various values of b, for comparison with the current obtained from the detailed numerical trajectory calculations. The agreement is excellent for b = 1 to within the accuracy of the numerical results. This may be connected with the fact that the numerical and analytic curves intersect the line 45.54 - z in trajectory space at very nearly the same value of z (at $z = z_1$), and that the structures of the curves for smaller values of z are probably unimportant since the integrand in Eq. (17) drops off very rapidly in

the vicinity of z_1. This situation might be expected to apply only to large values of V_o. However, as Fig. 8 shows, it apparently applies to small values of V_o as well.

Equation (35) shows that the slope of the current curve for large V_o is rather sensitive to the value of b. According to the arguments given above, b should be greater than unity. If it is only as large as 2, however, j/j_o remains less than 2 for all values of V_o, i.e., the one-dimensional limit is indicated. The theory is not applicable for values of b greater than 2, since Eq. (33) leads to negative values of j/j_o for large values of V_o.

The retarded current characteristic corresponding to the same allowed domain is obtained from Eqs. (21)-(23) by using $x_m(z)$ as given by Eq. (28) in Eq. (21), and with z_1 given by $b^2V_o/4$. Thus, the three possible cases may be expressed as:

(a) $0 \le V < b^2V_o/4$

$$\frac{j'}{j_o} = e^{V_o}\int_V^{b^2V_o/4} e^{-\frac{b^2V_o^2}{4z}}\,dz + 1 + V_o - \frac{b^2}{4}V_o$$

$$= 1 + V_o - V e^{-\frac{b^2V_o^2}{4V}+V_o} - \frac{b^2V_o^2}{4}e^{V_o}\left[E_1(V_o) - E_1\left(\frac{b^2V_o^2}{4V}\right)\right] \qquad (36)$$

where $E_1(\rho)$ denotes the exponential integral, Eq. (32).

(b) $b^2V_o/4 \le V \le V_o$

$$\frac{j'}{j_o} = V_o - V + 1 \qquad (37)$$

(c) $V > V_o$

$$\frac{j'}{j_o} = e^{V_o - V} \tag{38}$$

Equations (37) and (38) are identical to Eqs. (22) and (23) but are repeated here for completeness. The normalized retarded current j'/j_o is plotted in Fig. 6 for several values of b and $V_o = 45.54$. Equation (36) reduces to Eq. (33) for the total current when $V = 0$.

For large values of V_o, Eq. (36) has the asymptotic form:

$$\frac{j'}{j_o} \sim \left(1 + \frac{b^2}{4}\right) + \left(1 - \frac{b^2}{4}\right) V_o - \frac{4}{b^2} \frac{V^2}{V_o^2} e^{-V_o\left(\frac{b^2 V_o}{4V} - 1\right)} \tag{39}$$

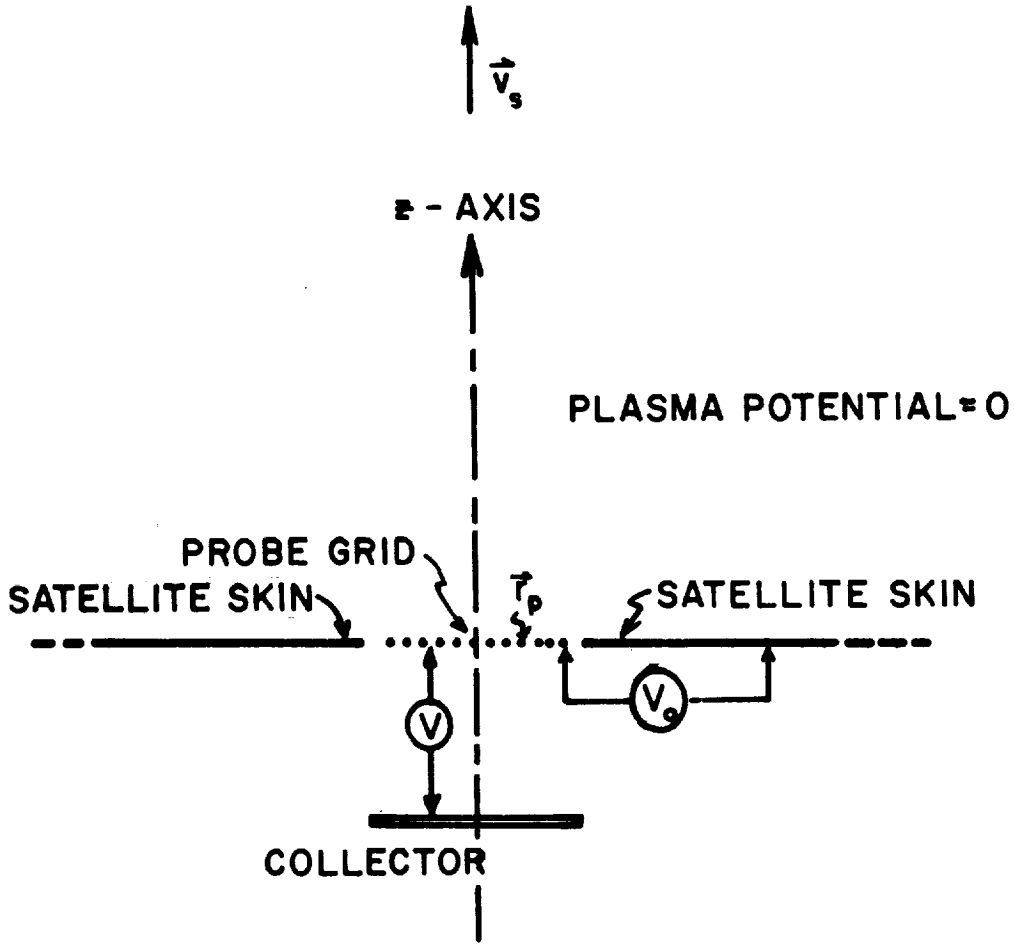

FIGURE 1. PLANAR PROBE GEOMETRY

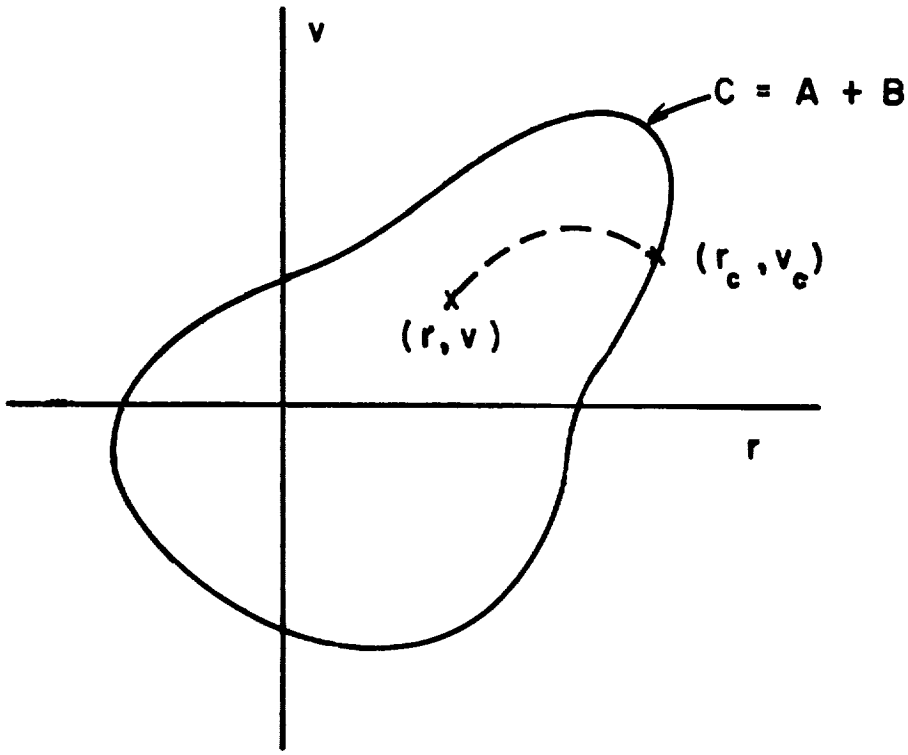

FIGURE 2. TWO DIMENSIONAL PHASE SPACE BOUNDARY. GENERAL.

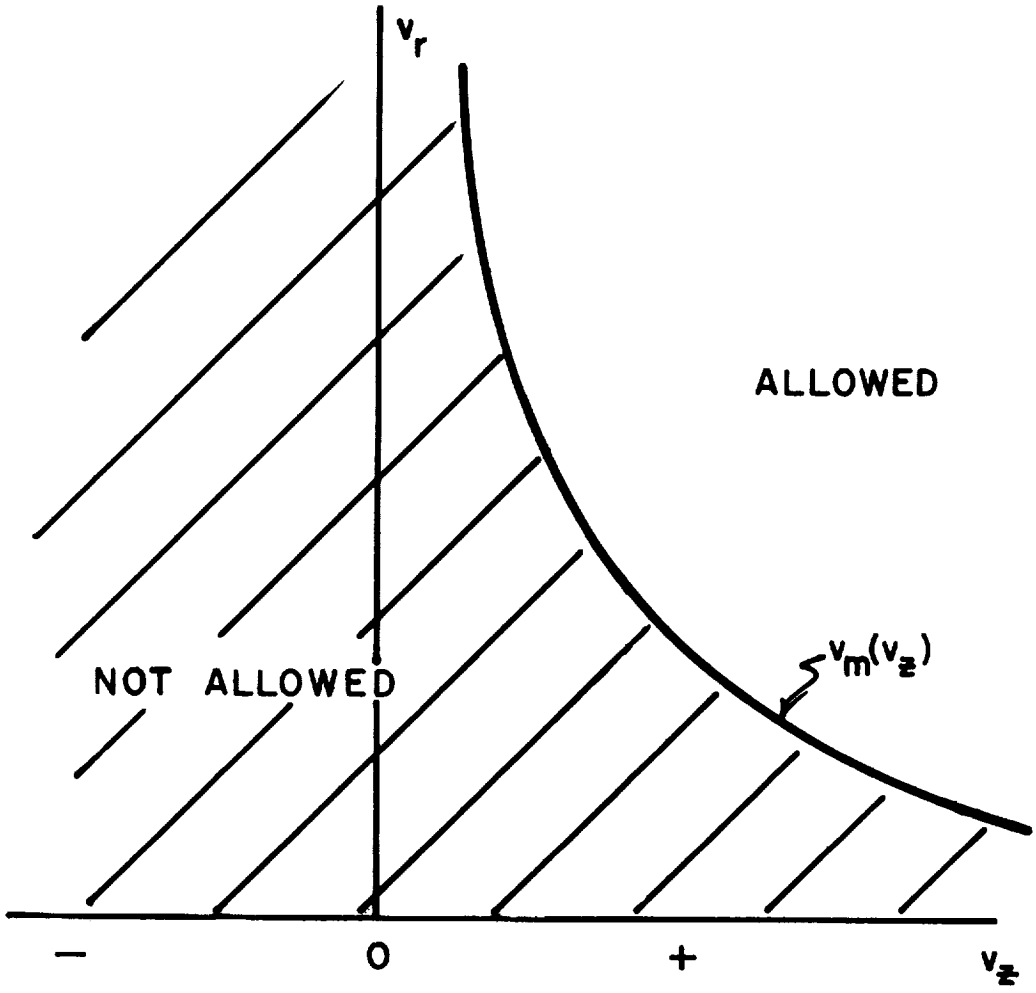

FIGURE 3. ALLOWED DOMAIN IN VELOCITY SPACE CORRESPONDING TO OCCUPIED TRAJECTORIES. GENERAL.

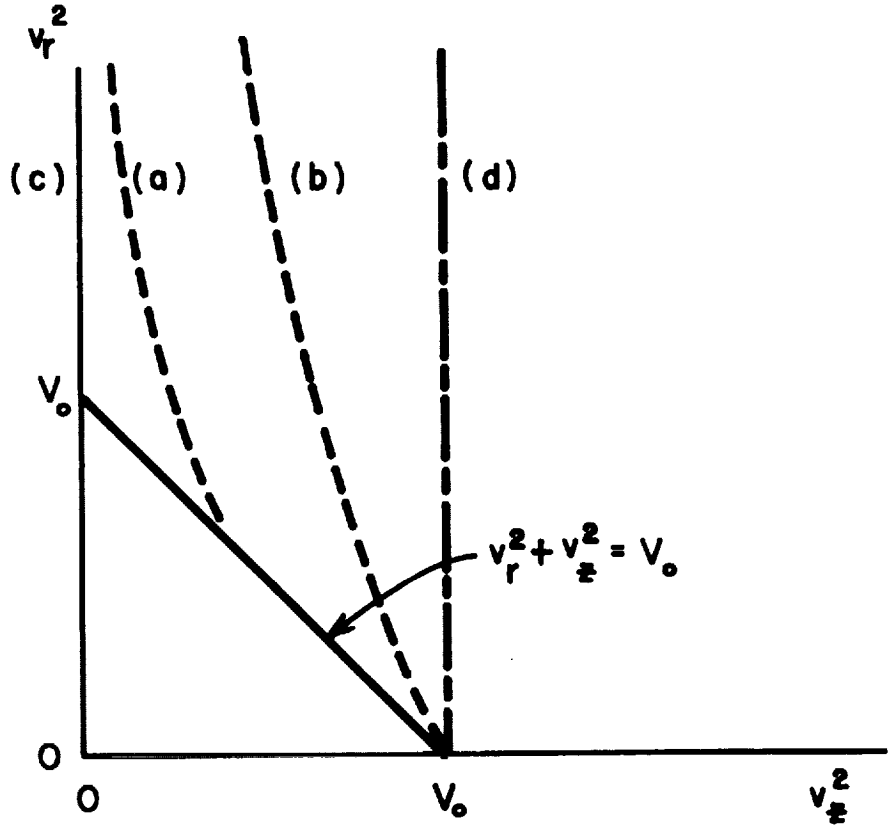

FIGURE 4. ALLOWED DOMAIN BOUNDARY IN TRAJECTORY SPACE. GENERAL.

(a) few intersections
(b) many intersections
(c) no intersections
(d) one-dimensional limit

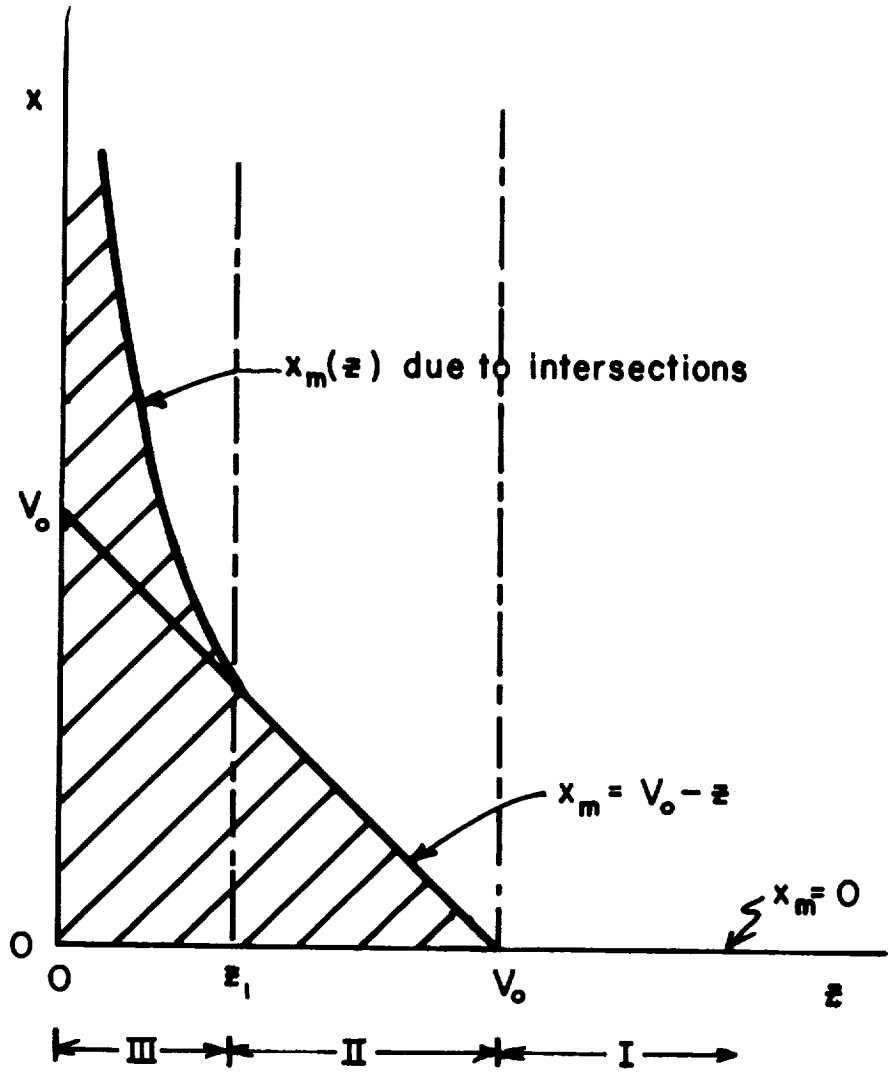

FIGURE 5. ALLOWED DOMAIN ASSUMED FOR PLANAR PROBE TRAJECTORY SPACE.

$(z = v_z^2, \quad x = v_r^2)$

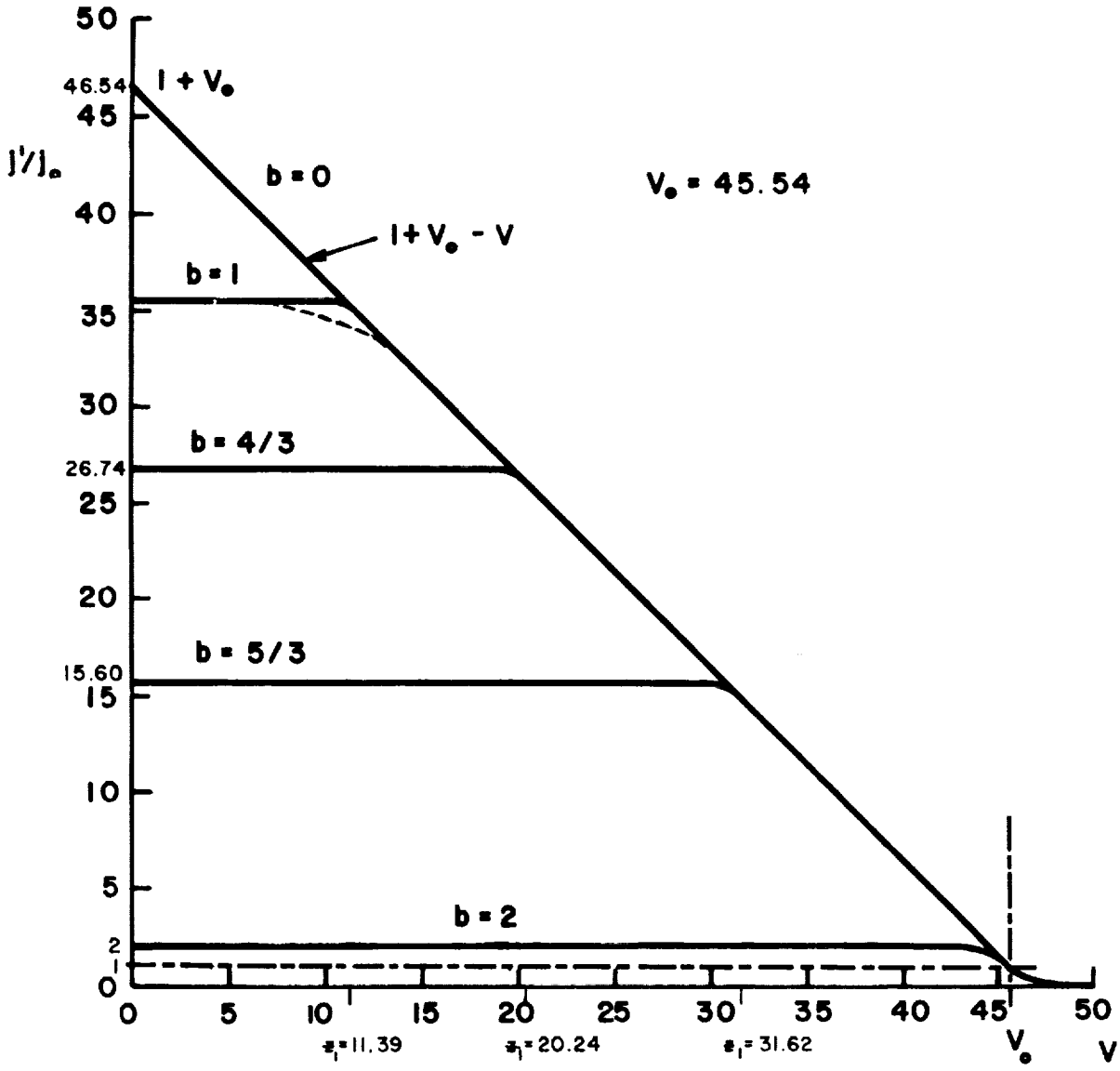

FIGURE 6. RETARDED CURRENT CHARACTERISTICS FOR ACCELERATING PLANAR PROBE. PARAMETER b FOR THEORETICAL MODEL.

(Dotted line numerically calculated, Fig. 10)

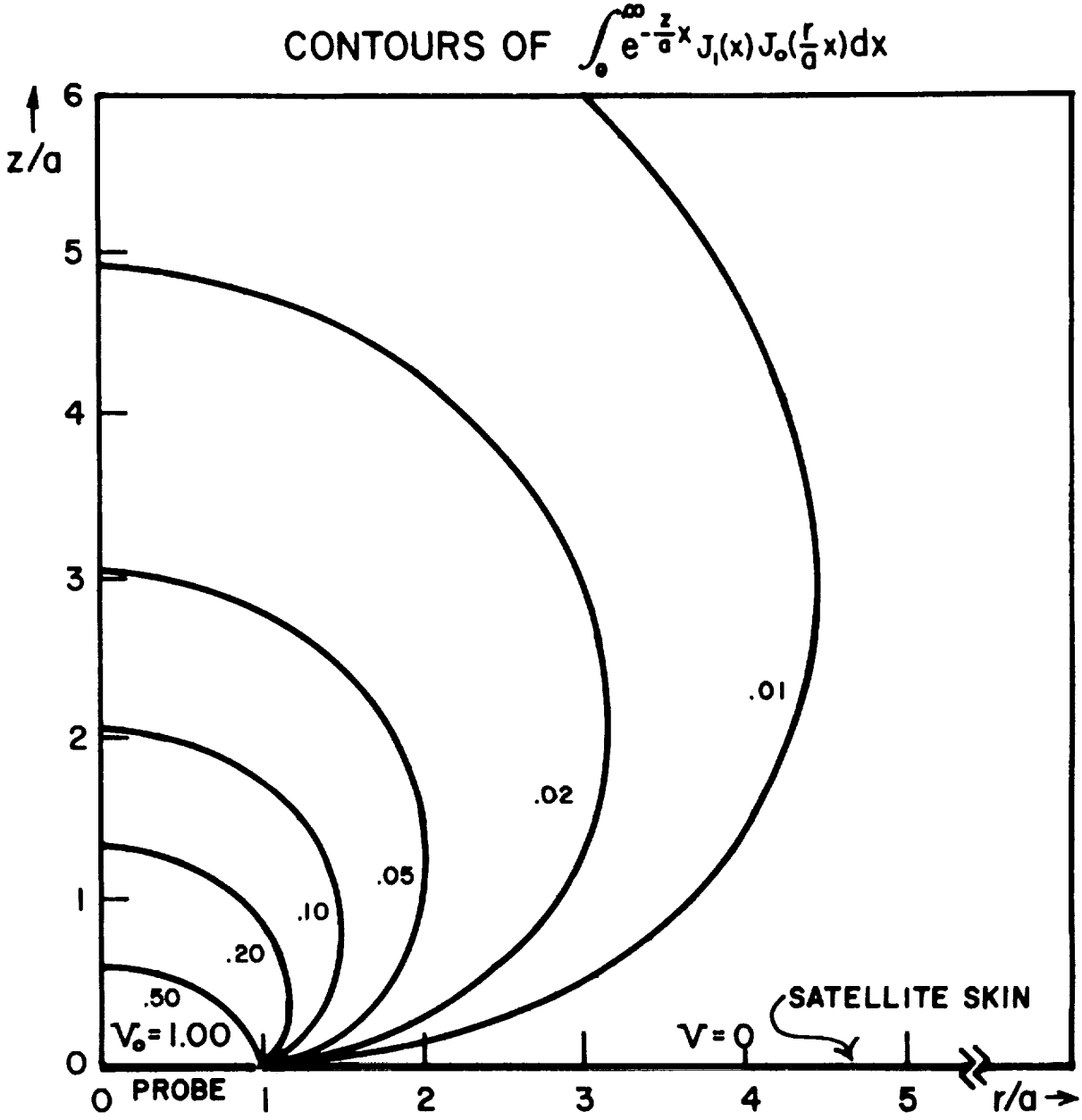

FIGURE 7. LAPLACE POTENTIAL FOR PLANAR PROBE

a = Probe Radius

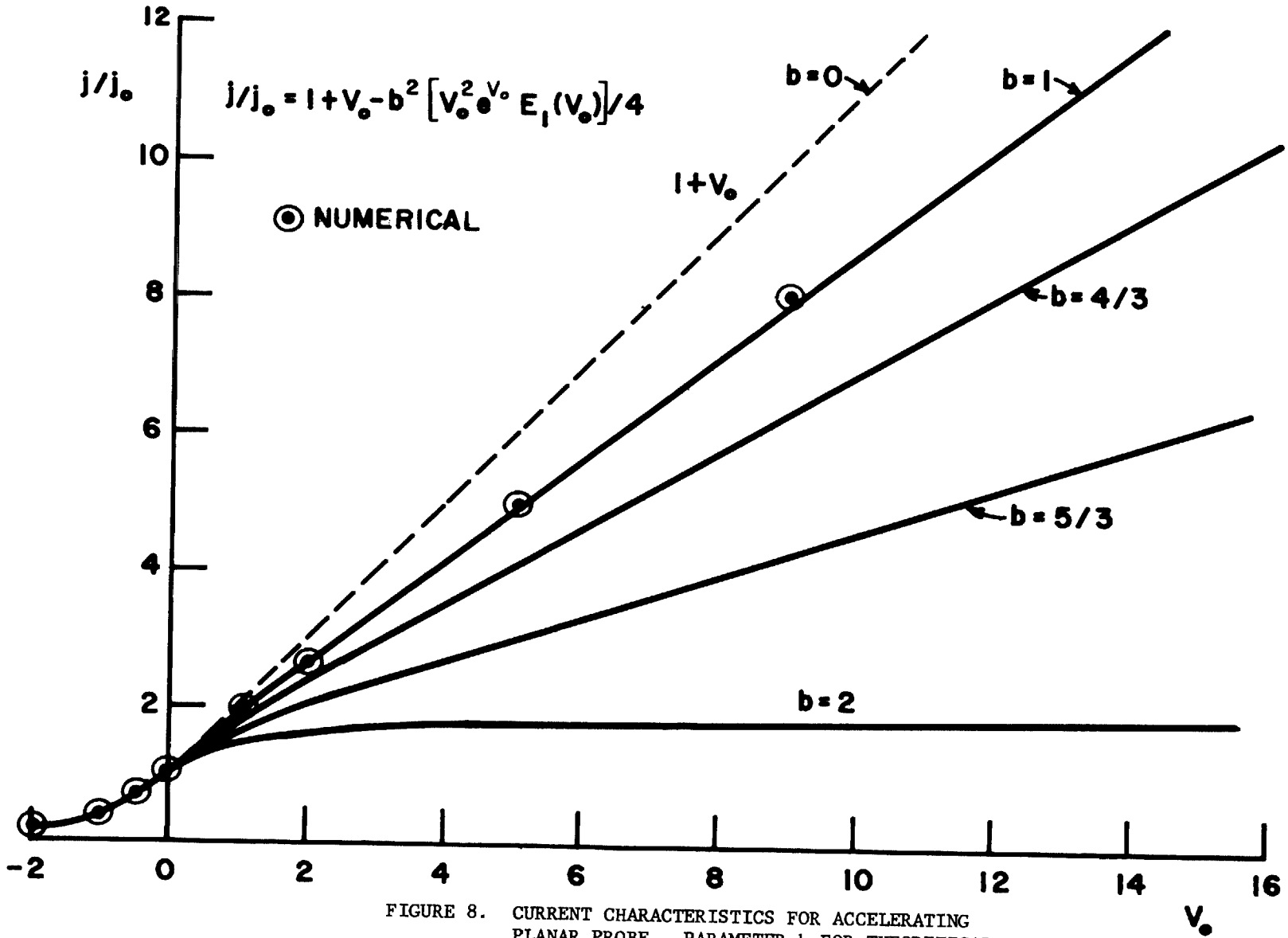

FIGURE 8. CURRENT CHARACTERISTICS FOR ACCELERATING PLANAR PROBE. PARAMETER b FOR THEORETICAL MODEL.

(Numerically Calculated Points in Circles)

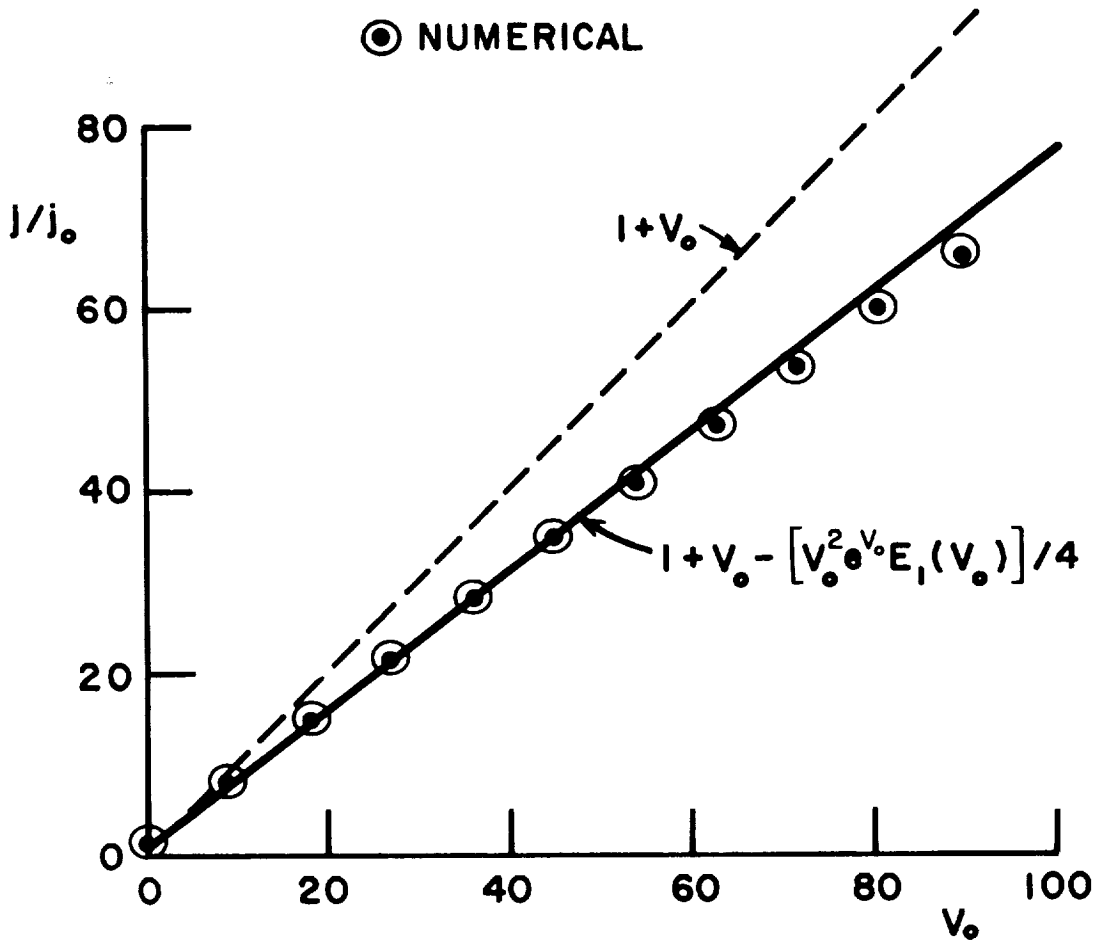

FIGURE 9. CURRENT CHARACTERISTIC FOR ACCELERATING PLANAR PROBE. LARGE VALUES OF V_o.
(Numerically Calculated Points in Circles)

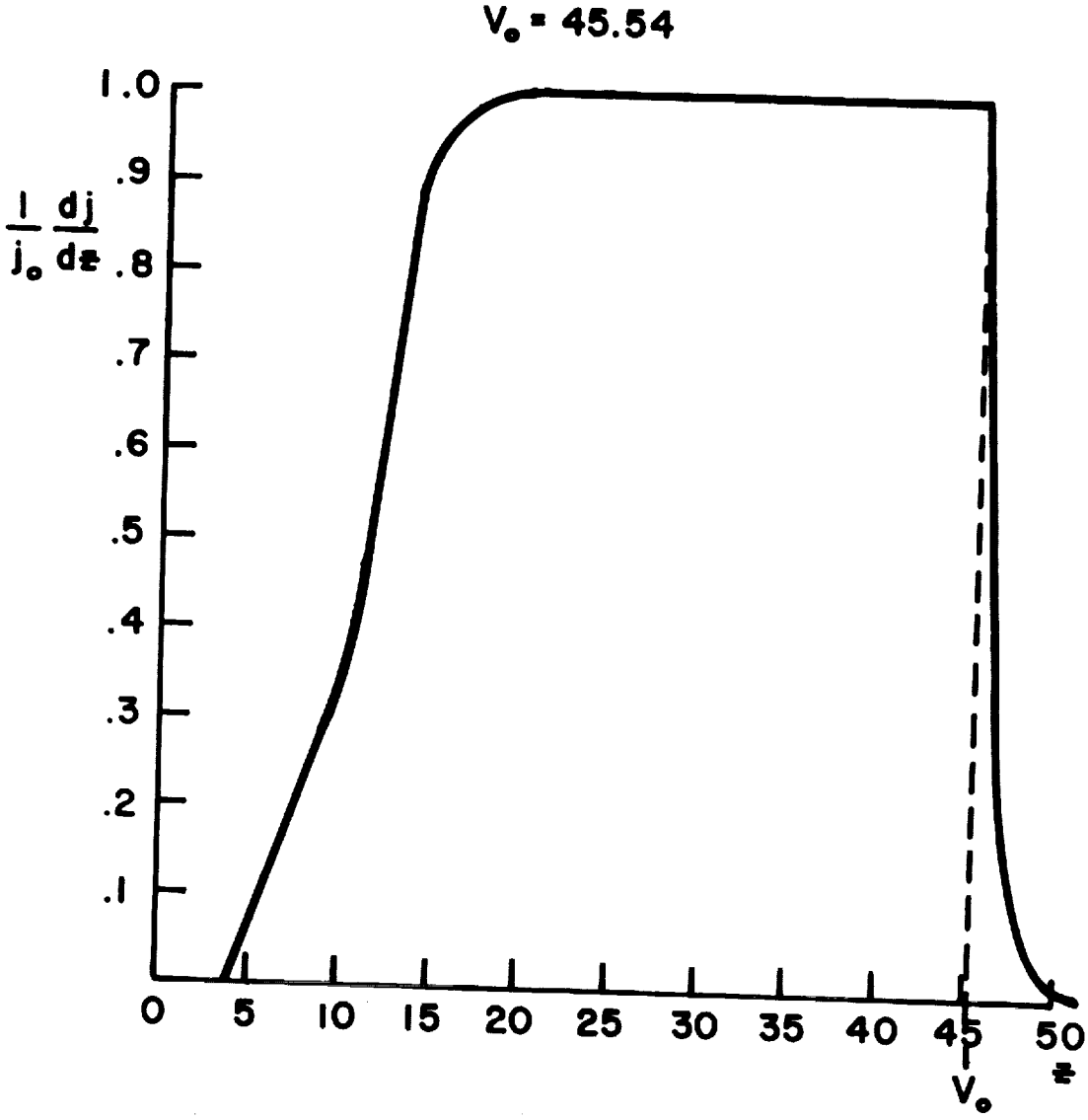

FIGURE 10. COMPUTED CURRENT DERIVATIVE WITH RESPECT TO KINETIC ENERGY ASSOCIATED WITH NORMAL COMPONENT OF VELOCITY.

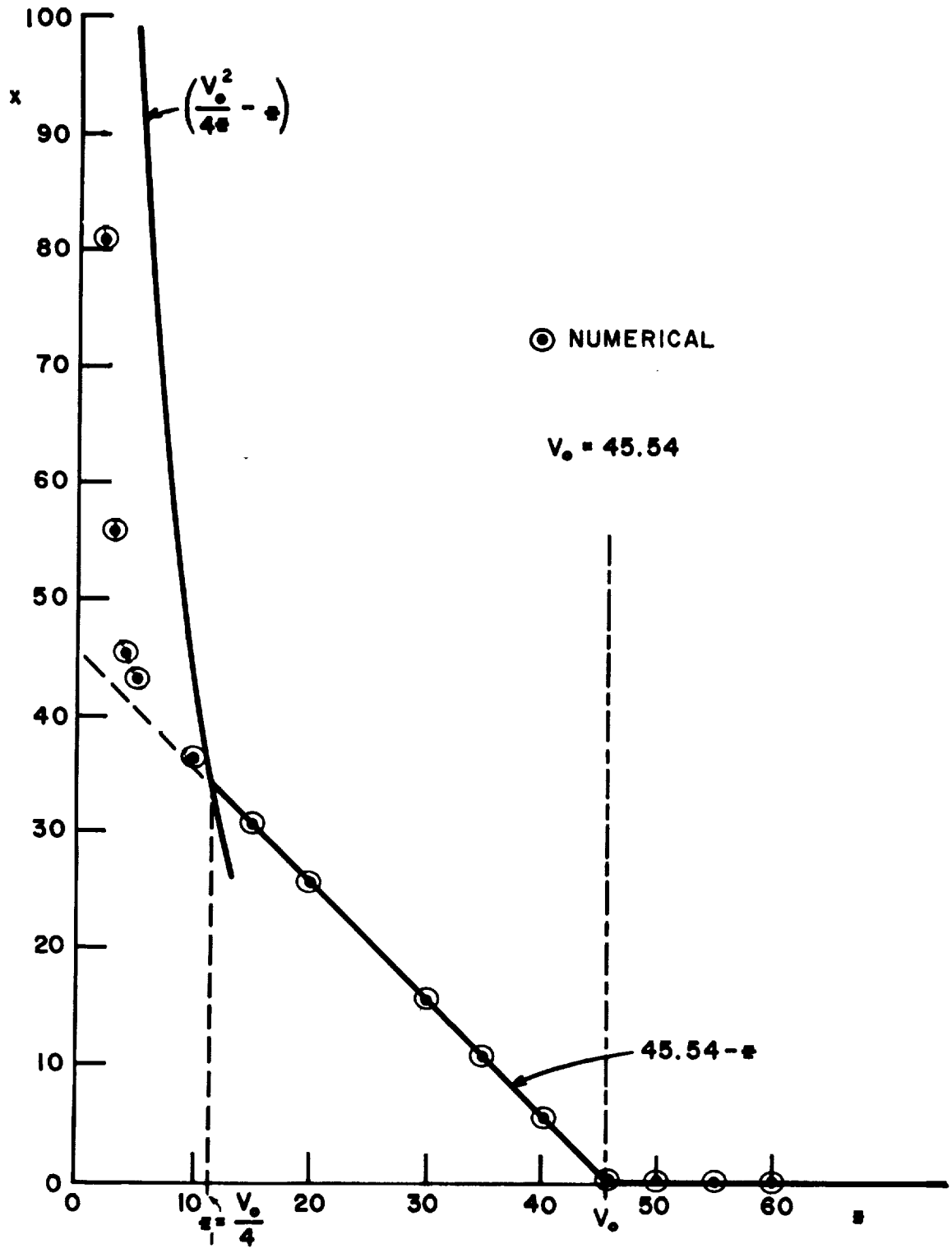

FIGURE 11. ALLOWED DOMAIN IN PLANAR PROBE TRAJECTORY SPACE. THEORETICAL VS COMPUTED CURVES. (Numerically Calculated Points in Circles)

APPENDIX A - INTERSECTIONS IN THE CASE OF A SPHERE

The material derived in this appendix is relevant to the subject of currect collection by spherical and cylindrical probes. The fact that a current limitation may be caused by the <u>form</u> of the potential distribution as well as the <u>value</u> of the probe potential has been considered by Hall[4], Bernstein and Rabinowitz[5], and Al'pert, Gurevich and Pitaevskii[6].

We assume that the potential distribution in the vicinity of a sphere which is embedded in a plasma may be described by the form

$$\Phi = - \frac{M}{r^n} \tag{A1}$$

where r is the radial distance from the center of the sphere and M and n are positive. It will be shown in this appendix that a grazing trajectory cannot exist at the surface of the sphere unless the exponent n is less than 2. A trajectory which can connect energetically with infinity will do so when n is less than 2, and may not connect with infinity (i.e., it may intersect) when n is greater than 2. In the latter case, intersections will limit the current which can be collected. An approximate expression for the current will be derived, with the exponent n as a parameter.

The equations of motion for a particle having mass m and angular momentum L, which is subjected to a potential energy function of the form Eq. (A1), are given by:

$$\ddot{r} = \frac{L^2}{m^2 r^3} - \frac{nM}{m r^{n+1}} \tag{A2}$$

$$\dot{\psi} = \frac{L}{mr^2} \tag{A3}$$

where the dots signify time-derivatives, r is the radial distance from the center of force, and ψ is the angle between the radius vector and an arbitrary reference line which lies in the plane of the orbit and passes through the center of force. With the use of the substitution

$$\frac{d}{dt} = \dot{\psi} \frac{d}{d\psi}$$

the differential equation for the orbit is:

$$\frac{d^2r}{d\psi^2} = \frac{2}{r}\left(\frac{dr}{d\psi}\right)^2 + r - \frac{nmMr^{3-n}}{L^2} \tag{A4}$$

Let the radius of the sphere be r_o, and consider a grazing trajectory at the point P as in Fig. A1. Let the angle ψ be measured from the line of symmetry O-P in Fig. A1. Expanding $r(\psi)$ about $\psi = 0$, we have, using Eq. (A4) and recalling that $(dr/d\psi)_o = 0$:

$$\frac{r}{r_0} = 1 + \frac{1}{2}\left(1 - \frac{nmV_o r_o^2}{L^2}\right)\psi^2 + \cdots \tag{A5}$$

where $V_o \equiv M / r_o^n = -\Phi(r_o)$

Thus, the radius of curvature of the trajectory is greater than r_o, as shown by the trajectory marked (a) in Fig. A1, if

$$V_o < \frac{L^2}{nmr_o^2} \quad \text{(no intersection)} \tag{A6}$$

and thus the trajectory does not intersect the sphere (at another point) and may possibly connect with infinity, depending on its energy. This inequality is automatically satisfied for a repulsive potential, since M, and therefore V_o, would be negative. For an attractive potential ($V_o > 0$), the inequality Eq. (A6) may or may not be satisfied. If it is not satisfied, i.e., if

$$V_o > \frac{L^2}{nmr_o^2} \quad \text{(intersection)} \tag{A7}$$

then the trajectory, as exemplified by (b) in Fig. A1, passes through the sphere. That is, the particle cannot have come from infinity, regardless of its energy.

The additional requirement that the trajectory must connect energetically with infinity may be expressed in terms of the local kinetic energy K. Thus, since

$$L^2 = 2mr_o^2 K \tag{A8}$$

and

$$K \geq V_o \quad \text{(attractive potential)} \tag{A9}$$

the criterion for a non-intersecting grazing trajectory which connects with infinity is obtained from Eq. (A6):

$$V_o < \frac{2mr_o^2}{nmr_o^2} K = \frac{2}{n} K \tag{A10}$$

or,

$$\frac{n}{2} V_o < K \quad \text{(no intersection)} \tag{A11}$$

If n is less than or equal to 2, Eq. (A11) is automatically satisfied (no intersection) when Eq. (A9) is satisfied (energetic connection with infinity). That is, Eq. (A9) is the appropriate criterion which includes Eq. (A11). Thus, the Langmuir formula for the current $j/j_o = 1 + V_o$ is obtained by integration over a Maxwellian distribution simply by considering Eq. (A9) for all trajectories, including grazing ones.

However, if n is greater than 2, Eq. (A11) is the appropriate criterion which includes Eq. (A9). Thus, an expression different from the Langmuir result would be obtained by using the correct formula for the boundary in trajectory space. This formula must reduce to Eq. (A11)

for grazing trajectories. In general, an exact analytic formula cannot be obtained. The charge density is also difficult to calculate when the potential falls off with r more rapidly than r^{-2}. Thus, the solution for the Poisson field in the vicinity of a sphere or cylinder embedded in a plasma has remained an extremely difficult problem to date.[4,5] However, it is possible to derive an approximate expression for the current when the exponent n is greater than 2. This may be of heuristic value.

Consider a trajectory which is not quite grazing (at the point P in Fig. A2), but is nearly so. In the vicinity of the point P, $r(\Psi)$ may be represented by the approximate expansion:

$$r(\Psi) = r_0 + \left(\frac{dr}{d\Psi}\right)_0 \Psi + \left[\frac{2}{r_0}\left(\frac{dr}{d\Psi}\right)_0^2 + r_0\left(1 - \frac{n m r_0^2 V_0}{L^2}\right)\right]\frac{\Psi^2}{2} \qquad \text{(A12)}$$

where use has been made of Eq. (A4). It will be assumed that retaining terms up to order Ψ^2 will give a sufficiently accurate representation of $r(\Psi)$, for a nearly grazing trajectory, to allow a conclusion to be drawn whether the trajectory intersects the sphere at another point (Q in Fig. A2). For very small displacement angles Ψ, the trajectory should be very nearly symmetrical about the point where r has its maximum value r_m. Differentiation of Eq. (A12) yields the following expression for Ψ_m, the angle corresponding to r_m:

$$\Psi_m \simeq -\left(\frac{dr}{d\Psi}\right)_0 \Big/ \left[\frac{2}{r_0}\left(\frac{dr}{d\Psi}\right)_0^2 + r_0\left(1 - \frac{n m r_0^2 V_0}{L^2}\right)\right] \qquad \text{(A13)}$$

Denoting by θ the angle made with the vertical at P by the particle velocity vector (see Fig. A2), we have the relation

$$\left(\frac{dr}{d\psi}\right)_o = r_o \cot\theta \tag{A14}$$

Moreover, using $L^2 = 2mr_o^2 K\sin^2\theta$, Eq. (A13) becomes:

$$\psi_m \simeq -K\sin\theta\cos\theta \Big/ \left[K\cos^2\theta + K - \frac{n}{2}V_o\right]$$

$$= v_r v_z \Big/ \left[\frac{n}{2}\left(\frac{2}{m}V_o\right) - 2v_z^2 - v_r^2\right] \tag{A15}$$

where v_r and v_z are the components of the particle velocity at P, perpendicular and parallel to the normal direction, respectively.

If the trajectory is not to intersect the sphere at any point Q, the angle ψ_m must be greater than some angle γ. This means that

$$\frac{m}{2}\left(v_r^2 + 2v_z^2 + \frac{v_r v_z}{\gamma}\right) > \frac{n}{2}V_o \tag{A16}$$

A simple formula results if γ is allowed to go to infinity, namely:

$$\frac{m}{2}v_r^2 > \frac{n}{2}V_o - m v_z^2 \tag{A17}$$

The assumption of an infinite rather than a finite value for γ is justified

within the present approximation. A finite value would complicate the algebra without introducing any qualitative changes in the conclusions.

In preparation for the use of Eq. (A17) to calculate the current for a Maxwellian distribution at infinity, let the velocities be expressed in units of $(2kT/m)^{\frac{1}{2}}$ and the energies in units of kT. Then, in accord with the notation of Section II and of Fig. 5, the allowed domain of integration is given by:

$2 \leq n \leq 4$

(I) $$\chi_m(z) = 0 \qquad (z > V_o) \tag{A18}$$

(II) $$\chi_m(z) = V_o - z \qquad (z_1 \leq z \leq V_o) \tag{A19}$$

(III) $$\chi_m(z) = \frac{n}{2} V_o - 2z \qquad (0 \leq z \leq z_1) \tag{A20}$$

where

$$z_1 \equiv \left(\frac{n}{2} - 1\right) V_o \tag{A21}$$

This domain in trajectory space is illustrated in Fig. A3.

The definition of the three regions in Eqs. (A18)-(A20) and Fig. A3 are in accord with Eq. (A17), when n is greater than 2 but less than 4. If n is greater than 4, the intercept on the z-axis by the straight line of Eq. (A20) lies at a value of z greater than V_o. This contradicts Eq. (A18), the justification of which has been discussed in Section II. However, the approximation above applies to nearly grazing trajectories, i.e., where n is slightly greater than 2, and z_1 (Eq. (A21)) is nearly zero. Hence, for $n > 4$, the domain is not correctly described

since the trajectories corresponding to the boundary of the domain, in Regions II and III, are far from grazing ones. The assumption will be made, therefore, that for $n > 4$, the allowed domain is given by:

$n > 4$

$$\text{(I)} \qquad \chi_m(z) = 0 \qquad (z > V_0) \tag{A22}$$

$$\text{(II,III)} \qquad \chi_m(z) = \frac{n}{2}(V_0 - z) \qquad (0 \le z \le V_0) \tag{A23}$$

The definition Eq. (A23) is illustrated by a dotted line in Fig. A3. The "patched up" equations, Eqs. (A22) and (A23), may not be grossly in error since Eq. (A23) gives the correct value $(n/2)V_0$ at the point $z = 0$, and the reasonable value, zero, at the point $z = V_0$.

On the basis of the allowed domain in the trajectory space defined by Eqs. (A18)-(A21) for $2 \le n \le 4$, and by Eqs. (A22)-(A23) for $n > 4$, Eq. (11) in Section II yields the following current density for a Maxwellian distribution:

$2 \le n \le 4$

$$\frac{j}{j_0} = e^{V_0}\left[\int_0^{(\frac{n}{2}-1)V_0} e^{-z-(\frac{n}{2}V_0 - 2z)}\,dz + \int_{(\frac{n}{2}-1)V_0}^{V_0} e^{-z-(V_0-z)}\,dz + \int_{V_0}^{\infty} e^{-z}\,dz\right]$$

$$= \left[1 - e^{-(\frac{n}{2}-1)V_0}\right] + (2 - \frac{n}{2})V_0 + 1 \tag{A24}$$

$$\underline{n > 4}$$

$$\frac{j}{j_o} = e^{V_o}\left[\int_o^{V_o} e^{-z - \frac{n}{2}(V_o - z)}\, dz + \int_{V_o}^{\infty} e^{-z}\, dz\right]$$

$$= \frac{1}{\left(\frac{n}{2}-1\right)}\left[1 - e^{-\left(\frac{n}{2}-1\right)V_o}\right] + 1 \qquad \text{(A25)}$$

where $j_o = n_o(kT/2\pi m)^{\frac{1}{2}}$ (Equation (10) in Section II). The behavior of the current density as a function of V_o, with the exponent n as a parameter, is illustrated in Fig. A4. For V_o near zero, all of the curves behave like $1 + V_o$, independent of n. For n between 2 and 4, the asymptotic behavior of the current is linear, with slope (2-n/2) varying between unity and zero as a function of n. For n greater than 4, an apparent "saturation" is manifested. However, this saturation effect is quantitatively doubtful due to the approximations used, but is perhaps qualitatively reasonable. It corresponds to the one-dimensional limit where intersections are dominant. (See Reference 6, p. 230.)

The retarded current characteristic corresponding to the same allowed domain is obtained by suitably modifying the limits on the integrals in Eqs. (A24) and (A25). If the potential barrier to be overcome by the collected particles is V, we have the following cases:

$$\underline{\text{(a)}\ \ 2 \le n \le 4 \quad \text{and} \quad 0 \le V < \left(\tfrac{n}{2}-1\right)V_o}$$

$$\frac{j'}{j_o} = e^{V_o}\int_V^{\left(\frac{n}{2}-1\right)V_o} e^{z - \frac{n}{2}V_o}\, dz + 1 + \left(2 - \tfrac{n}{2}\right)V_o$$

$$= \left[1 - e^{-\left(\frac{n}{2}-1\right)V_o + V}\right] + 1 + \left(2 - \tfrac{n}{2}\right)V_o \qquad \text{A26)}$$

(b) $2 \le n \le 4$ and $\left(\frac{n}{2}-1\right)V_o \le V \le V_o$

$$\frac{j'}{j_o} = e^{V_o}\int_V^{V_o} e^{-V_o}\,dz + 1 = V_o - V + 1 \qquad \text{(A27)}$$

(c) $2 \le n \le 4$ and $V > V_o$

$$\frac{j'}{j_o} = e^{V_o}\int_V^{\infty} e^{-z}\,dz = e^{V_o - V} \qquad \text{(A28)}$$

(d) $n > 4$ and $0 \le V \le V_o$

$$\frac{j'}{j_o} = e^{V_o}\left[\int_V^{V_o} e^{-\frac{n}{2}V_o + \left(\frac{n}{2}-1\right)z}\,dz + \int_{V_o}^{\infty} e^{-z}\,dz\right]$$

$$= \frac{1}{\left(\frac{n}{2}-1\right)}\left[1 - e^{-\left(\frac{n}{2}-1\right)(V_o - V)}\right] + 1 \qquad \text{(A29)}$$

(e) $n > 4$ and $V > V_o$

$$\frac{j'}{j_o} = e^{V_o}\int_V^{\infty} e^{-z}\,dz = e^{V_o - V} \qquad \text{(A30)}$$

The retarded current characteristic is plotted in Fig. A5, for $V_o = 45.54$, for values of n = 2, 2.5, 3, 3.5, 4, and 6.

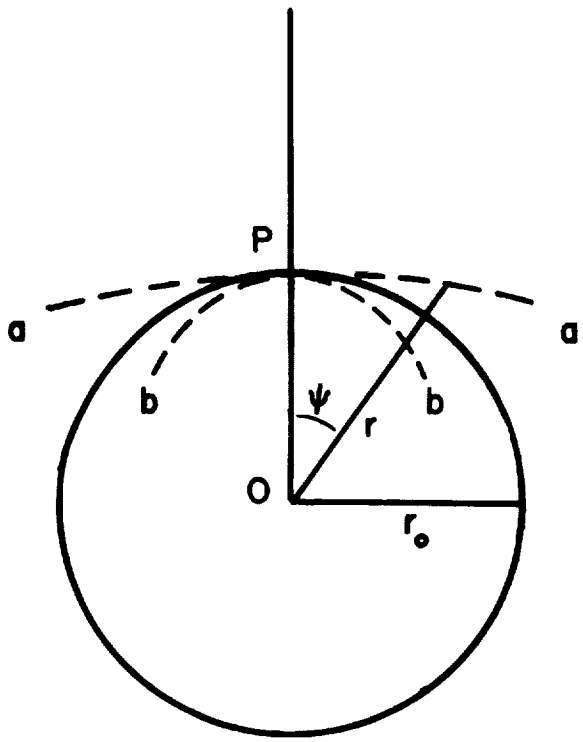

FIGURE A1. GRAZING TRAJECTORIES

(a) Radius of Curvature > r_o

(b) Radius of Curvature < r_o

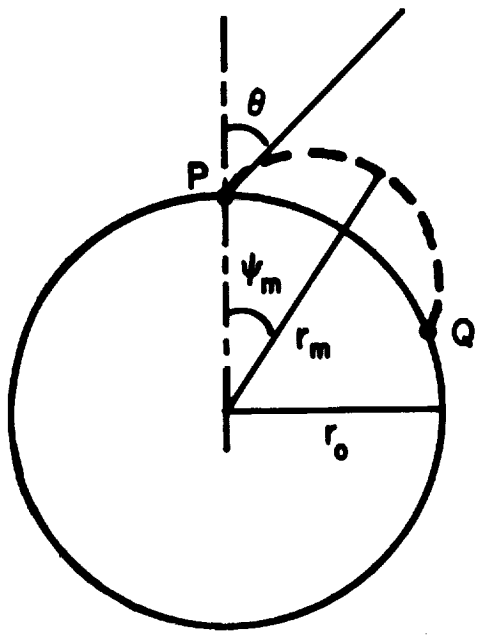

FIGURE A2. NEARLY-GRAZING INTERSECTING TRAJECTORIES

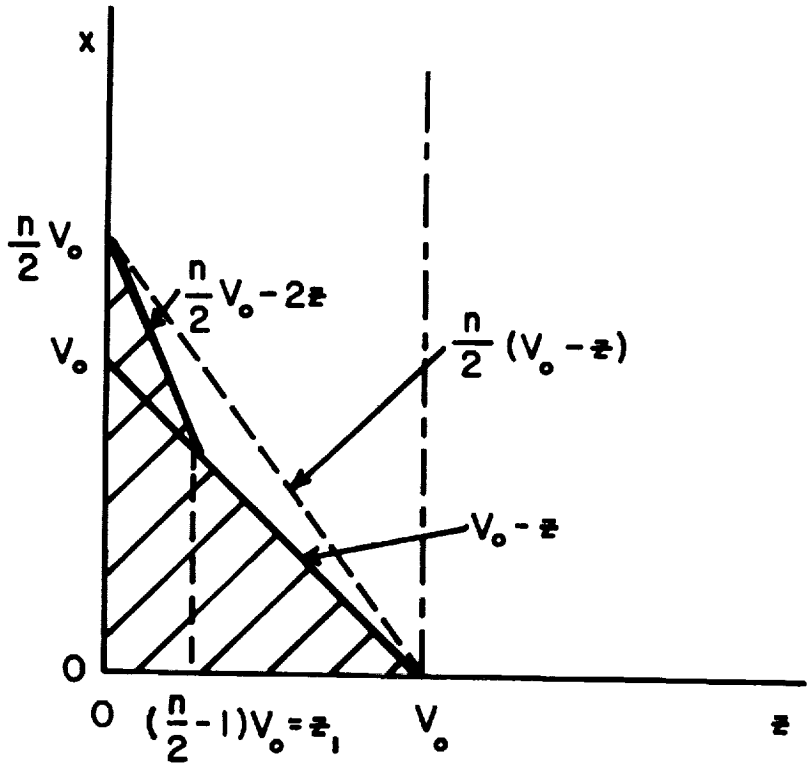

FIGURE A3. SPHERICALLY SYMMETRIC POWER-LAW POTENTIAL. ALLOWED DOMAIN IN TRAJECTORY SPACE.

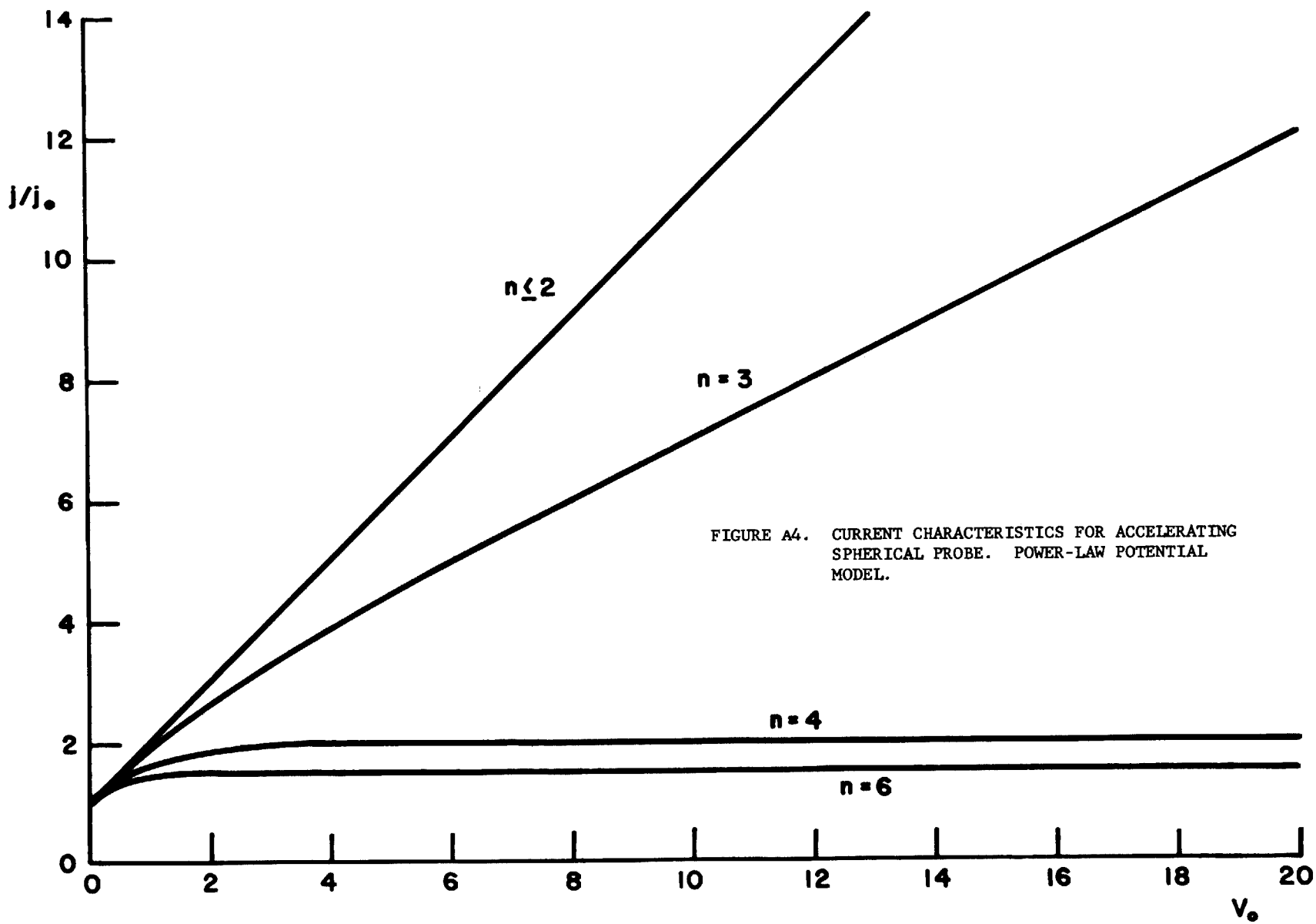

FIGURE A4. CURRENT CHARACTERISTICS FOR ACCELERATING SPHERICAL PROBE. POWER-LAW POTENTIAL MODEL.

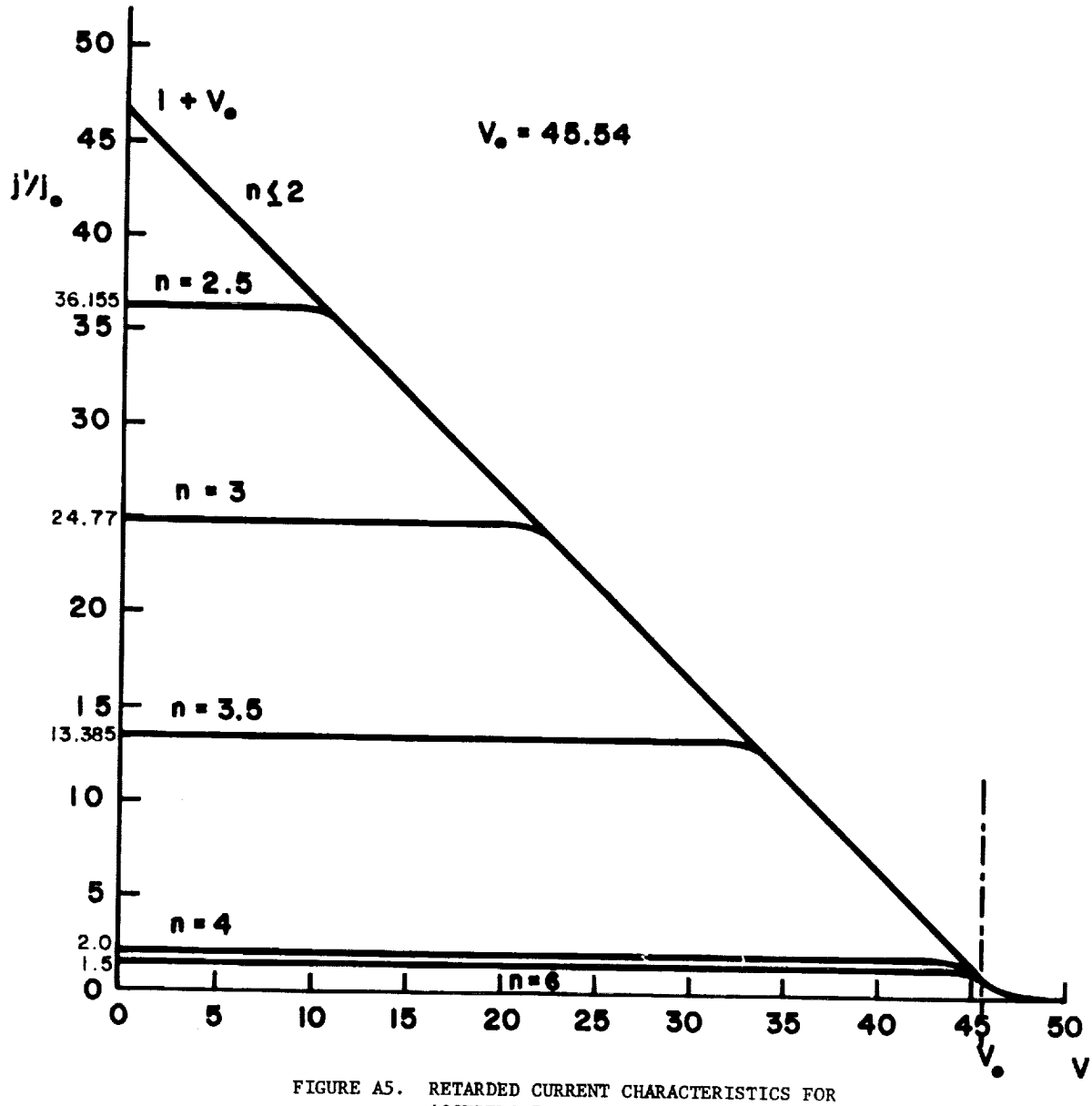

FIGURE A5. RETARDED CURRENT CHARACTERISTICS FOR ACCELERATING SPHERICAL PROBE. POWER-LAW POTENTIAL MODEL.

APPENDIX B - DRUYVESTEYN RELATIONS FOR ISOTROPIC DISTRIBUTIONS

When the Boltzmann distribution function or density in phase space corresponds to an isotropic velocity distribution at infinity, the current density of particles incident at a point on the surface of the probe may be expressed by:

$$j = 2\pi \iint f_\infty \left(v_\infty^2\right) v_z \, dv_z \, v_r \, dv_r \tag{B1}$$

where f_∞ is the Boltzmann distribution function. In Eq. (B1), the geometry is assumed symmetric about the normal direction, and v_z and v_r denote components of velocity parallel and perpendicular to this direction, respectively. Let z and x denote v_z^2 and v_r^2, respectively, for convenience.

Consider first the grid of the probe to be biased at a repulsive potential so that the particles of interest must overcome a potential energy barrier of height V in order to be collected from infinity. Assume that the collecting electrode is biased so as to attract all particles passing through the grid. Then

$$j = \frac{\pi}{2} \iint f_\infty \left(x + z + \frac{2}{m} V\right) dz \, dx \tag{B2}$$

where m is the particle mass, and energy conservation has been invoked. Since the energy requirement is that x + z be positive or zero, the entire x - z plane is energetically allowed. Assuming no exclusion due to intersections, we may write:

$$j = \frac{\pi}{2} \int_0^\infty dz \int_0^\infty dx \, f_\infty \left(x + z + \frac{2}{m} V\right) \tag{B3}$$

By transforming to new variables, z and u = x + z + (2/m)V, we have

$$j(V) = \frac{\pi}{2}\int_0^\infty dz \int_{z+\frac{2}{m}V}^\infty du\, f_\infty(u) = \frac{\pi}{2}\int_{\frac{2}{m}V}^\infty (u - \tfrac{2}{m}V) f_\infty(u)\, du \quad \text{(B4)}$$

where the last form was obtained by interchanging the order of integration. Thus, by differentiating once with respect to V, we obtain

$$\frac{dj}{dV} = -\frac{\pi}{m}\int_{\frac{2V}{m}}^\infty f_\infty(u)\, du \quad \text{(B5)}$$

And by a second differentiation with respect to V, we obtain

$$\frac{d^2j}{dV^2} = \frac{2\pi}{m^2} f_\infty\left(\tfrac{2}{m}V\right) \quad \text{(B6)}$$

Equation (B6) may be considered as one form of the Druyvesteyn relation. Let the speed distribution at infinity be denoted by $\rho_\infty(v_\infty)$, such that $\rho_\infty(v_\infty)dv_\infty$ gives the number of particles per unit volume which have speeds lying in the interval dv_∞. Then the relation between f_∞ and ρ_∞ is

$$f_\infty(v_\infty^2) = \frac{1}{4\pi v_\infty^2}\rho_\infty(v_\infty) \quad \text{(B7)}$$

so that Eq. (B6) can be put in the form:

$$\frac{d^2j}{dV^2} = \frac{2\pi}{m^2}\frac{1}{4\pi}\frac{m}{2V}\rho_\infty\left(\sqrt{2V/m}\right) = \frac{1}{4mV}\rho_\infty\left(\sqrt{2V/m}\right) \quad \text{(B8)}$$

which is the formula given by Druyvesteyn[2]. (See also Reference 3, p. 753.)

Now consider the probe grid to be biased at an attractive potential so that particles coming from infinity have at least a kinetic energy V_o at the probe. As before, let the collecting electrode be biased so as to attract all particles passing through the grid. Then the current density is given by

$$j = \frac{\pi}{2} \iint f_\infty \left(x + z - \frac{2}{m} V_o \right) dz\, dx \tag{B9}$$

The energy requirement is that $x + z - \frac{2}{m} V_o$ be positive or zero. Hence, the energetically excluded domain of the x - z plane is the triangle near the origin bounded by the lines $x = 0$, $z = 0$, and $x + z = (2/m)V_o$. Assuming no additional exclusion due to intersections, we may write:

$$j = \frac{\pi}{2} \int_0^{\frac{2}{m}V_o} dz \int_{\frac{2}{m}V_o - z}^{\infty} dx\, f_\infty \left(x + z - \frac{2}{m} V_o \right) + \frac{\pi}{2} \int_{\frac{2}{m}V_o}^{\infty} dz \int_0^{\infty} dx\, f_\infty \left(x + z - \frac{2}{m} V_o \right) \tag{B10}$$

By transforming to new variables, z and $u = x + z - (2/m)V_o$, we have

$$j = \frac{\pi}{2} \int_0^{\frac{2}{m}V_o} dz \int_0^{\infty} du\, f_\infty(u) + \frac{\pi}{2} \int_{\frac{2}{m}V_o}^{\infty} dz \int_{z - \frac{2}{m}V_o}^{\infty} du\, f_\infty(u) \tag{B11}$$

or

$$j = c V_o + d \tag{B12}$$

where c and d are constant moments of the distribution function, namely:

$$c = \frac{\pi}{m} \int_0^\infty f_\infty(u)\, du \tag{B13}$$

$$d = \frac{\pi}{2} \int_0^\infty f_\infty(u)\, u\, du \tag{B14}$$

The form of Eq. (B14) may be obtained from the second term of Eq. (B11) by reversing the order of integration. In the case of the Maxwellian distribution, i.e., where f_∞ is given by

$$f_\infty(u) = n_o \left(\frac{m}{2\pi kT}\right)^{3/2} e^{-\frac{mu}{2kT}} \tag{B15}$$

the constants c and d become:

$$c = (n_o / kT)\left(\frac{kT}{2\pi m}\right)^{1/2}$$

$$d = n_o \left(\frac{kT}{2\pi m}\right)^{1/2} \tag{B16}$$

Thus, for the attracting probe the resulting linear relation Eq. (B12) bears no resemblance to the distribution function, and a Druyvesteyn relation does not exist.

Now let the collecting electrode be biased so as to repel particles passing through the grid, and let the potential energy difference between the grid and the collector be denoted by V. Then the current equation Eq. (B11) is modified as follows. When V is less than V_o,

$$j = \frac{\pi}{2} \int_{\frac{2}{m}V}^{\frac{2}{m}V_o} dz \int_0^\infty du\, f_\infty(u) + d = c(V_o - V) + d \qquad \text{(B17)}$$

where c and d are defined by Eqs. (B13) and (B14). The lower limit on the z-integration is raised from 0 to (2/m)V since only values of z greater than or equal to (2/m)V at the probe grid can contribute to the current collected. Again, due to the linear form of Eq. (B17) there exists no Druyvesteyn relation for $V < V_o$.

However, when V is greater than V_o, the first term in Eq. (B11) makes no contribution at all, and the second term is modified to yield:

$$j = \frac{\pi}{2} \int_{\frac{2}{m}V}^{\infty} dz \int_{z - \frac{2}{m}V_o}^{\infty} du\, f_\infty(u)$$

$$= \frac{\pi}{2} \int_{\frac{2}{m}(V - V_o)}^{\infty} \left[u - \frac{2}{m}(V - V_o) \right] f_\infty(u)\, du \qquad \text{(B18)}$$

which follows upon reversing the order of integration. Equation (B18) becomes identical to Eq. (B4) if V - V_o is replaced by V. Hence a Druyvesteyn relation exists and the analysis following Eq. (B4) for the case of a repelling probe may be carried through in an identical fashion. Thus, defining $\Delta V \equiv V - V_o$, we have, according to Eqs. (B5), (B6), and (B8):

$$\frac{dj}{d\Delta V} = -\frac{\pi}{m}\int_{\frac{2}{m}\Delta V}^{\infty} f_{\infty}(u)\,du \tag{B19}$$

$$\frac{d^2j}{d\,\Delta V^2} = \frac{2\pi}{m^2} f_{\infty}(2\,\Delta V/m) \tag{B20}$$

$$\frac{d^2j}{d\,\Delta V^2} = \frac{1}{4m\,\Delta V} \rho_{\infty}(-\sqrt{2\,\Delta V/m}) \tag{B21}$$

Therefore, the case of the attracting probe with an internal repelling collector is equivalent to the case of the repelling probe, since in either case, a Druyvesteyn relation holds with respect to the net repulsive potential barrier which the particles must overcome in coming from infinity to the collector.

According to the discussion of Section II, exclusions in x - z space due to intersections of trajectories with the satellite surface are not likely to modify the boundary for $z > V_o$. Thus, when V is greater than V_o, Eqs. (B18)-(B21) remain valid in the presence of intersection effects.

APPENDIX C - EFFECTS OF INTERSECTIONS FOR GENERAL ISOTROPIC DISTRIBUTIONS

The equations in Appendix B have been derived on the assumption that no part of trajectory space is excluded because of intersections. They are applicable to any geometry, provided that it is rotationally symmetric. Intersection effects, if present, will be manifested in the current characteristic of an accelerating probe and will depend on the geometry of the probe. In exploring the modifications in the characteristic caused by intersections for arbitrary isotropic distributions, we will first consider the case of a sphere, which has already been treated in Appendix A for the case of a Maxwellian distribution. We will employ the exponent n of Appendix A as a parameter to characterize the spherical potential distribution. Following this, we will similarly consider the planar probe characteristics, which have been treated in Section IV for a Maxwellian distribution. We will use the parameter b of Section IV to characterize the potential distribution. For both the sphere and planar probe, the limits on the integrals in Eqs. (B10)-(B11) of Appendix B will be modified.

SPHERE

Assuming that the exponent n, which characterizes the spherically symmetric potential distribution lies between 2 and 4, the allowed domain of integration in trajectory space may be obtained from Eqs. (A18)-(A21) of Appendix A as follows:

$2 \leq n \leq 4$

(I) $\chi_m = 0 \qquad \left(z > \frac{2}{m} V_o \right)$ (C1)

(II) $\chi_m = \frac{2}{m} V_o - z \qquad \left(z_1 \leq z \leq \frac{2}{m} V_o \right)$ (C2)

(III) $\chi_m = \frac{n}{m} V_o - 2z \qquad \left(0 \leq z < z_1 \right)$ (C3)

where

$$z_1 \equiv \left(\frac{n}{2} - 1 \right) \frac{2}{m} V_o \tag{C4}$$

In Eqs. (C1)-(C4), x and z denote v_r^2 and v_z^2, respectively, in cylindrical velocity coordinates, V_o is the potential energy of the attracted particles at the sphere surface, and m is the particle mass.

Thus, instead of Eq. (B11) of Appendix B we have:

$$j = \frac{\pi}{2}\int_0^{z_1} dz \int_{z_1 - z}^{\infty} du\, f_\infty(u)$$

$$+ \frac{\pi}{2}\int_{z_1}^{\frac{2}{m}V_0} dz \int_0^{\infty} du\, f_\infty(u)$$

$$+ \frac{\pi}{2}\int_{\frac{2}{m}V_0}^{\infty} dz \int_{z - \frac{2}{m}V_0}^{\infty} du\, f_\infty(u) \qquad \text{(C5)}$$

By reversing the order of integration in the first and last terms, we may rewrite Eq. (C5) as follows:

$$\frac{j}{j_o} = \frac{\pi}{2d}\int_0^{z_1} f_\infty(u)\, u\, du$$

$$+ \frac{\pi}{2d} z_1 \int_{z_1}^{\infty} f_\infty(u)\, du$$

$$+ \frac{c}{d}\left(2 - \frac{n}{2}\right)V_o \quad + \quad 1 \qquad \text{(C6)}$$

where $z_1 = (n - 2)V_o/m$, and where c and d are the moment integrals defined by Eqs. (B13) and (B14) of Appendix B, respectively. When the potential V_o is zero, j is equal to d, which may be also designated as j_o. Thus, the normalized current ratio j/j_o may be obtained by division by d. For the case of a Maxwellian distribution, i.e., where $f_\infty(u)$, c, and d are given by Eqs. (B15) and (B16) of Appendix B, we recover the ratio j/j_o as given by Eq. (A24) of Appendix A, namely:

$$\frac{j}{j_o} = \left[1 - e^{-\left(\frac{n}{2}-1\right)\frac{V_o}{kT}}\right] + \left(2 - \frac{n}{2}\right)\frac{V_o}{kT} + 1 \qquad \text{(C7)}$$

Taking the derivative with respect to V_o of j/j_o as given by the general relation, Eq. (C6), we obtain:

$$\frac{d}{dV_o}\left(\frac{j}{j_o}\right) = \frac{1}{d}\left[c\left(2 - \frac{n}{2}\right) + \frac{\pi}{m}\left(\frac{n}{2} - 1\right)\int_{z_1}^{\infty} f_\infty(u)\,du \right] \quad \text{(C8)}$$

where $z_1 = (n - 2)V_o/m$.

By a second differentiation with respect to V_o, we obtain:

$$\frac{d^2}{dV_o^2}\left(\frac{j}{j_o}\right) = -\frac{\pi(n-2)^2}{2m^2 d} f_\infty\left[\frac{(n-2)}{m} V_o\right] \quad \text{(C9)}$$

Thus, a Druyvesteyn relation exists for the accelerating spherical probe due to the presence of intersections ($n > 2$). Since n is not known, Eq. (C9) cannot be used for the determination of f_∞. If f_∞ is known, however, Eq. (C9) might be useful for determining n, i.e., the characteristic parameter for the field around the probe.

It is interesting to apply the foregoing equations to the case of a monoenergetic distribution, for comparison with the Maxwellian. Letting f_∞ be given by the delta-function

$$f_\infty(u) = A\,\delta(u - u_o) \quad \text{(C10)}$$

where A is a constant, the normalized current ratio obtained from Eq. (C6) may be written:

$$c = \frac{\pi}{m} A$$

$$d = \frac{\pi}{2} u_o A$$

$$\frac{j}{j_o} = \frac{1}{u_o} \int_0^{z_1} \delta(u-u_o)\, u\, du \quad + \quad \frac{z_1}{u_o} \int_{z_1}^{\infty} \delta(u-u_o)\, du$$

$$+ \left(2 - \frac{n}{2}\right) \frac{2V_o}{m u_o} \quad + \quad 1 \qquad \text{(C11)}$$

where $z_1 = (n - 2)V_o/m$. There are two ranges to be considered, according as z_1 is greater or less than u_o. Thus, denoting by φ the ratio $2V_o/mu_o$, we obtain:

(a) $\varphi < \frac{2}{n-2}$

$$\frac{j}{j_o} = 1 + \varphi \qquad \text{(C12)}$$

(b) $\varphi > \frac{2}{n-2}$

$$\frac{j}{j_o} = 2 + \left(2 - \frac{n}{2}\right)\varphi \qquad \text{(C13)}$$

In case (a) the first integral of Eq. (C11) vanishes, while in case (b) the second integral vanishes. Both Eqs. (C12) and (C13) are linear, but with different slopes. The discontinuity in slope occurs for $\varphi = 2/(n-2)$, where $j/j_o = n/(n-2)$. Considering j/j_o as a function of $\varphi \equiv 2V_o/mu_o$, the slope is unity for the lower range of φ, and between unity and zero for the upper range of φ, depending on the value of n. The existence of a discontinuity in the slope of the accelerating probe current characteristic for a monoenergetic distribution has been suggested by Medicus[10] on the basis of qualitative arguments regarding the sheath thickness. (The variation of the parameter n here may be regarded equivalently as a variation in sheath thickness.) This phenomenon occurs only for a delta-function, in which case the second term in Eq. (C8) becomes a step function. For a continuous distribution, however, the derivative is continuous. It is evident, by comparison of Eqs. (C7) and (C13), that the slope of the asymptotic straight line approached for large values of V_o is the same for the Maxwellian and monoenergetic distributions, when the characteristics are considered as functions of the appropriate dimensionless variables.

PLANAR PROBE

In the case of the planar probe, the allowed domain of integration in trajectory space may be written, using the theory of Sections II and IV, as follows:

$$\text{(I)}\quad \chi_m = 0 \qquad \left(z > \frac{2}{m} V_0\right) \tag{C14}$$

$$\text{(II)}\quad \chi_m = \frac{2}{m} V_0 - z \qquad \left(z_1 \le z \le \frac{2}{m} V_0\right) \tag{C15}$$

$$\text{(III)}\quad \chi_m = \frac{b^2 V_0^2}{m^2 z} - z \qquad \left(0 \le z < z_1\right) \tag{C16}$$

where

$$z_1 \equiv b^2 V_0 / 2m \tag{C17}$$

In Eqs. (C14)-(C17), x and z denote v_r^2 and v_z^2, respectively, V_0 is the potential energy of the attracted particles at the probe grid, and m is the particle mass.

Then Eq. (B11) of Appendix B becomes:

$$j = \frac{\pi}{2}\int_0^{z_1} dz \int_{\left(\frac{z_1}{z}-1\right)\frac{2}{m}V_0}^{\infty} du\, f_\infty(u) \;+\; \frac{\pi}{2}\int_{z_1}^{\frac{2}{m}V_0} dz \int_0^{\infty} du\, f_\infty(u)$$

$$+\; \frac{\pi}{2}\int_{\frac{2}{m}V_0}^{\infty} dz \int_{z-\frac{2}{m}V_0}^{\infty} du\, f_\infty(u) \qquad \text{(C18)}$$

where $z_1 = b^2 V_0/2m$.

By reversing the order of integration in the first and last terms, we may write Eq. (C18) as follows:

$$j = \frac{\pi}{2} z_1 \int_0^{\infty} \frac{du\; u\, f_\infty(u)}{\left(u + \frac{2}{m}V_0\right)} \;+\; \frac{\pi}{2}\left(\frac{2}{m}V_0 - z_1\right)\int_0^{\infty} du\, f_\infty(u)$$

$$+\; \frac{\pi}{2}\int_0^{\infty} du\; u\, f_\infty(u) \qquad \text{(C19)}$$

Now $j_o = j(V_o = 0)$. Hence, defining

$$j_o \equiv \frac{\pi}{2} \int_0^\infty du\ u\ f_\infty(u) \tag{C20}$$

and

$$c \equiv \frac{\pi}{2} \int_0^\infty du\ f_\infty(u) \tag{C21}$$

we may express the normalized current ratio as:

$$\frac{j}{j_o} = \frac{\pi}{2}\ \frac{z_1}{j_o} \int_0^\infty \frac{du\ u\ f_\infty(u)}{\left(u + \frac{2}{m} V_o\right)}$$

$$+ \left(1 - \frac{b^2}{4}\right) \frac{2 V_o}{j_o m}\, c \quad + \quad 1 \tag{C22}$$

For the case of a Maxwellian distribution, where $f_\infty(u) = A \exp(-mu/kT)$, we have $c = \pi A kT/m$, $j_o = 2\pi A k^2 T^2/m^2$, and Eq. (C22) yields:

$$\frac{j}{j_o} = 1 + \frac{V_o}{kT} - \left(\frac{b V_o}{2kT}\right)^2 e^{\frac{V_o}{kT}}\, E_1\left(\frac{V_o}{kT}\right) \tag{C23}$$

in accord with Eq. (33) of Section IV. The constant A, which is $n_o (m/2\pi kT)^{3/2}$, is immaterial since it appears in both numerator and denominator of the terms of Eq. (C22).

For the case of a monoenergetic distribution, where $f_\infty(u) = A\,\delta(u - u_o)$, we have $c = \pi A/2$, $j_o = \pi A u_o/2$, and Eq. (C22) yields

$$\frac{j}{j_o} = 1 + \varphi - \frac{b^2}{4}\,\frac{\varphi^2}{1+\varphi} \qquad \text{(C24)}$$

where φ denotes the ratio $2V_o/mu_o$.

It is interesting to note that the planar probe current characteristic for the monoenergetic distribution given by Eq. (C24) is continuous and has continuous derivatives, in contrast to the case of the spherical probe (Eqs. (C12)-(C13)). Comparison of Eqs. (C23) and (C24) shows that the asymptotic linear behavior is the same, when j/j_o is considered as a function of the appropriate dimensionless variable.

By taking derivatives of the general characteristic given by Eq. (C22), one does not obtain a Druyvesteyn relation for the planar probe as is found for the spherical probe. (See Eq. (C9).)

APPENDIX D - SPECIAL CASE OF A MOVING SPHERICAL PROBE WITH SPHERICALLY SYMMETRIC POTENTIAL

Although it is not possible in general to express in analytic form the current to a moving probe, an exceptional case occurs for a spherical probe when the potential distribution about the probe is spherically symmetric.

The case where the potential is spherically symmetric and the velocity distribution is a Maxwellian with a superimposed drift velocity has been treated in recent years[10,11]. Work has also been performed on the problem of a cylindrical probe in the same velocity distribution[3,12]. In these problems the concept of a sheath of finite thickness was employed to characterize the potential distribution function.

We have already treated the case of a spherical probe in a Maxwellian velocity distribution in Appendix A, and a general isotropic distribution in Appendix C. In these Appendices we have introduced a new model, namely, that of a power-law potential characterized by an exponent n, which was employed to take into account trajectory exclusions due to intersections. In this Appendix we will extend the theory of Appendices A and C to the case where the particle velocity distribution in the plasma is any rotationally symmetric function, the most important example being an isotropic function with a superimposed drift velocity. The method, however, can be applied to any velocity distribution whatsoever. The potential distribution function will be assumed to have a fixed spherically symmetric form, despite the presence of a distribution of space charge which is not spherically symmetric. When the plasma is extremely rarefied, space charge effects should produce a negligible distortion of the potential from spherical symmetry. At the same time, the deviation of the potential from the Laplace (Coulomb) form should also be small. When the plasma is not rarefied, the deviation from spherical symmetry due to the presence of space charge would be small if the drift velocity is small. For sufficiently

small drift velocities, then, or for sufficiently rarefied plasmas, the spherically symmetric approximation may be a good one and may yield fruitful results[3,10,11]. We will therefore proceed, under the assumption of spherical symmetry, to examine the effects of the form of the distribution function, and of trajectory exclusions due to intersections, on the current characteristics of the spherical probe.

Although it is simpler to use directly the angular momentum or impact parameter approach[10,11] to derive the integral for the probe current, we will employ the equivalent approach of performing an integration of the local current density over the surface of the sphere. That is, we will preserve the formulation of this report, in which the current density is obtained by an integration over the local velocity space at a point on the surface of the sphere. This formulation may have value in permitting one to examine the collection of current in the neighborhood of such a point. However, for the purpose of this report, we will not consider individual points, but will take full advantage of symmetry in performing the surface integral. The velocity distribution at infinity will be assumed to have rotational symmetry about an axis, but it will be clear from the results that the formula for the current will be applicable to any velocity distribution whatever, provided that the appropriate <u>speed</u> distribution is used. A Druyvesteyn relation holds, for the retarding sphere, between the second derivative of the potential and the speed distribution.

The integral to be derived for the current to the accelerating sphere will be shown to have a general form which may be applied to any mathematical model describing the effects of trajectory exclusions. Thus, it is of interest to obtain an expression for the current based on the power-law potential model of Appendix A, and to compare this with the current based on the sheath model[3,10,11]. For a Maxwellian velocity distribution with superimposed drift, it will be shown that the two models have similar properties, so that they are in a sense equivalent.

The current collected by a sphere may be written in the form

$$I = \iint_{\text{sphere}} d^2\Sigma \iiint_{\text{occupied}} f(\vec{r}, \vec{v})\,(\vec{v}\cdot\hat{n})\,d^3\vec{v} \qquad \text{(D1)}$$

where $d^2\Sigma$ is the element of surface of the sphere, $\hat{n}$ is a unit vector in the direction of the outward normal at the surface element, and f is the distribution function, i.e., the density in phase space. The outward normal direction is considered positive for convenience. Since the trajectories are to be followed backwards in time to their origin, it is convenient to consider only outgoing velocity vectors and to reverse the velocities at infinity for the evaluation of the distribution function.

For a rotationally symmetric velocity distribution with an axis of symmetry along the direction of a unit vector $\hat{v}_s$, the distribution function for occupied trajectories (see Section II for the definition of the term "occupied") may be written:

$$f(\vec{r}, \vec{v}) = f_\infty(v_\infty, \cos\psi_\infty) \tag{D2}$$

where ψ_∞ is the angle made by the particle velocity vector ($\vec{v}_\infty$) with the direction of $\hat{v}_s$ at infinity. The quantity v_∞ is the speed at infinity, which is related to the local speed (v) by

$$v_\infty^2 = v^2 + \frac{2}{m}\Phi \tag{D3}$$

where Φ is the local potential energy of the particle and m is its mass. For example, an isotropic velocity distribution with a superimposed drift velocity $\vec{v}_s$ may be represented by the function

$f_\infty(v_\infty^2 + v_s^2 - 2v_\infty v_s \cos\psi_\infty)$, i.e., by a function of the single argument $(\vec{v}_\infty - \vec{v}_s)^2$.

The following coordinate system will be adopted; as illustrated in Fig. D1. The point at which the current density is to be evaluated is the point P, located on a sphere of radius r_o, at a polar angle ξ with respect to the principal axis, $\hat{v}_s$. The outward normal unit vector at this point is $\hat{n}$. The primed velocity coordinates v_x', v_y' , v_z' refer to a coordinate system fixed in space, with the v_z'-axis along the direction of $\hat{v}_s$, and the v_x'-axis perpendicular to this axis and lying in the plane containing the vectors $\hat{v}_s$ and $\hat{n}$. The

v_y'-axis is perpendicular to this plane. The unprimed velocity coordinates v_x, v_y, v_z refer to a coordinate system which rotates with the vector $\hat{n}$, where the v_z-axis is along the direction of $\hat{n}$, the v_x-axis is perpendicular to this axis (tangent to the sphere at P) and lying in the $\hat{n}$ - $\hat{v}_s$ plane, and the v_y-axis is parallel to the v_y'-axis. Thus, the unprimed coordinate system may be obtained from the primed coordinate system by a rotation about the v_y-axis through an angle ξ.

Let $\vec{v}$ be the local velocity vector at the point P. It is convenient to introduce spherical polar velocity coordinates, i.e. v, θ', φ' and v, θ, φ for the primed and unprimed systems, respectively. Here, θ' is the polar angle made by the velocity vector $\vec{v}$ with the $\hat{v}_s$-axis, and φ' is the azimuthal angle made by the $\vec{v}$-$\hat{v}_s$ plane with the $\hat{n}$ - $\hat{v}_s$ plane. The angle θ is the polar angle made by $\vec{v}$ with the $\hat{n}$-axis, and φ is the azimuthal angle made by the $\vec{v}$ - $\hat{n}$ plane with the $\hat{n}$ - $\hat{v}_s$ plane. The angle φ is equal to 0 (or π) when $\vec{v}$ is in the $\hat{n}$ - $\hat{v}_s$ plane and headed away from (or toward) the positive $\hat{v}_s$ -axis.

The trajectory passing through the point P is associated with a particle having the velocity vector $\vec{v}_\infty$ at infinity. In the primed coordinate system, the vector $\vec{v}_\infty$ makes a polar angle θ_∞' with the $\hat{v}_s$ -axis and φ_∞' is the azimuthal angle, which is equal to φ' for a spherically symmetric potential. In the unprimed coordinate system, the vector $\vec{v}_\infty$ makes a polar angle θ_∞ with the $\hat{n}$-axis, and φ_∞ is the azimuthal angle, which is equal to φ for a spherically symmetric potential. The angles θ, θ_∞, and θ_∞' are shown in Fig. D1.

Thus, we have the following relations between the angles in the two coordinate systems:

$$\sin\theta'\cos\varphi' = \cos\xi \sin\theta \cos\varphi + \sin\xi \cos\theta \tag{D4}$$

$$\sin\theta'\sin\varphi' = \sin\theta \sin\varphi \tag{D5}$$

$$\cos\theta' = -\sin\xi \sin\theta \cos\varphi + \cos\xi \cos\theta \tag{D6}$$

Since the angle ψ_∞ which enters into Eq. (D2) is the supplement of θ'_∞, we obtain from Eq. (D6) the relation

$$\cos\psi_\infty = \sin\xi \sin\theta_\infty \cos\varphi - \cos\xi \cos\theta_\infty \tag{D7}$$

In Eq. (D7), θ_∞ may be defined as the change in polar angle of the particle in going from the point P to infinity. It is a function of θ and v, but not of φ, and may be expressed by the following formula when the potential is proportional to r^{-n}:

$$\theta_\infty = \sin\theta \int_0^1 \left[1 - \sin^2\theta\, x^2 + (1-x^n)\frac{2\Phi(r_0)}{mv^2} \right]^{-\frac{1}{2}} dx \tag{D8}$$

In terms of the angles defined above, the five-dimensional integral for the current, Eq. (D1) may be written as

$$I = 2\pi r_0^2 \int_{v_{min}}^{\infty} v^3 dv\; G(v, \Phi_0) \tag{D9}$$

The lower limit on the v-integral depends on the sign of Φ_0 and will be discussed later.

In Eq. (D9), G is defined by

$$G(\vec{v}, \Phi_0) = \int_0^{\pi} \sin\xi \, d\xi \int_0^{\theta_{max}} \sin\theta\cos\theta \, d\theta \int_0^{2\pi} d\varphi$$

$$\cdot \, f_\infty\left(v_\infty, \sin\xi \sin\theta_\infty \cos\varphi - \cos\xi \cos\theta_\infty\right) \tag{D10}$$

where Φ_0 is the potential energy of the particle at the sphere surface, and the function f_∞ has been defined as in Eq. (D2). In deriving Eq. (D9), use has been made of the symmetry about the direction of $\hat{v}_s$ in the surface integration. The upper limit θ_{max} on the θ-integral depends on intersection effects, which will be discussed later.

It is now convenient to transform the integration over ξ to an integration over $\cos\psi_\infty$, where $\cos\psi_\infty$ is defined by Eq. (D7) as the second argument in the distribution function f_∞. From Eq. (D7) we find $\cos\xi$ as a function of $\cos\psi_\infty$:

$$\cos\xi = \frac{-\cos\theta_\infty \cos\psi_\infty \pm \sin\theta_\infty \cos\varphi \sqrt{\cos^2\theta_\infty + \sin^2\theta_\infty \cos^2\varphi - \cos^2\psi_\infty}}{\cos^2\theta_\infty + \sin^2\theta_\infty \cos^2\varphi} \tag{D11}$$

Note that there are two branches in the transformation, given by the two signs. The Jacobian of the transformation is

$$\frac{\partial \cos\xi}{\partial \cos\psi_\infty} = -T_1 \mp T_2 \tag{D12}$$

where

$$T_1 = \frac{\cos\theta_\infty}{\cos^2\theta_\infty + \sin^2\theta_\infty \cos^2\varphi} \tag{D13}$$

$$T_2 = \frac{\sin\theta_\infty \cos\psi_\infty \cos\varphi}{(\cos^2\theta_\infty + \sin^2\theta_\infty \cos^2\varphi)\sqrt{\cos^2\theta_\infty + \sin^2\theta_\infty \cos^2\varphi - \cos^2\psi_\infty}} \tag{D14}$$

Thus, we may write the function G as

$$G(v, \Phi_0) = \int_0^{\pi} \sin\psi_\infty d\psi_\infty f_\infty(v_\infty, \cos\psi_\infty) \int_0^{\theta_{max}(v)} \sin\theta \cos\theta \, d\theta$$

$$\cdot \int d\varphi \; (-T_1 \mp T_2) \tag{D15}$$

where the range of the φ-integration will now be discussed.

Considering θ, and therefore θ_∞, fixed, the range of φ is taken from 0 to 2π provided that the radicand of Eqs. (D11) or (D14) does not vanish for any value of φ in this range. In this case, the integration over T_2 gives zero, and the integration over T_1 gives simply 2π, independent of θ_∞. Either branch of the transformation may be chosen, and no transfer occurs from one branch to the other. However, if the radicand vanishes for a value of φ, designated by φ_m, then the range of φ is restricted in such a way that the radicand remains positive. The argument is too lengthy to be given here, but it may be shown that a transfer occurs from one branch to the other as φ passes through the value φ_m. In this case, the integration over T_2 gives 2π, while the integration over T_1 gives zero.

Thus, ignoring the sign of the Jacobian, the function G becomes:

$$G(v, \Phi_0) = \pi \sin^2\theta_{max} \int_0^{\pi} f_\infty(v_\infty, \cos\psi_\infty) \sin\psi_\infty \, d\psi_\infty \qquad \text{(D16)}$$

and the current becomes, using Eq. (D9):

$$I = 2\pi^2 r_0^2 \int_{v_{min}}^{\infty} \sin^2\theta_{max} \, v^3 dv \int_0^{\pi} f_\infty(v_\infty, \cos\psi_\infty) \sin\psi_\infty d\psi_\infty \qquad \text{(D17)}$$

With the use of Eq. (D3), the v-differential may be transformed by

$$v^3 dv = \left(v_\infty^2 - \frac{2}{m}\Phi_0\right) v_\infty \, dv_\infty \tag{D18}$$

into the differential of the speed at infinity. The resulting current may be written:

$$I = \pi r_0^2 \int_{v_{\infty min}}^{\infty} \sin^2\theta_{max} \left(v_\infty^2 - \frac{2}{m}\Phi_0\right) \frac{N(v_\infty)}{v_\infty} \, dv_\infty \tag{D19}$$

where $N(v_\infty)$ is the speed distribution defined by:

$$N(v_\infty) \equiv 2\pi v_\infty^2 \int_0^{\pi} f_\infty(v_\infty, \cos\psi_\infty) \sin\psi_\infty \, d\psi_\infty \tag{D20}$$

The differential $N(v_\infty)\,dv_\infty$ represents the number of particles per unit volume at infinity which have speeds lying in the range v_∞ to $v_\infty + dv_\infty$. The symbol N appears here in a manner identical to that in which the symbol ρ_∞ appears in Appendix B. (See Eq. (B7) in Appendix B.) In Appendix B, ρ_∞ denotes the speed distribution in an isotropic velocity distribution. The symbol N will be associated with a more general velocity distribution.

In Eq. (D19), $v_{\infty min}$ is given by zero or $(2\Phi_o/m)^{\frac{1}{2}}$, according as Φ_o is negative or positive, respectively.

If $\Phi_o = V$, where V is positive, the probe is retarding and there are no trajectory exclusions due to intersections. (See Section II for definitions of terms.) Therefore, θ_{max} has the constant value $\pi/2$, and a Druyvesteyn relation follows from Eq. (D19). With $v_{\infty min} = (2V/m)^{\frac{1}{2}}$, the second derivative of I with respect to V is given by

$$\frac{d^2I}{dV^2} = 4\pi r_o^2 \cdot \frac{1}{4mV} N\left(\sqrt{2V/m}\right) \tag{D21}$$

where N is defined by Eq. (D20). (Compare Eq. (D21) with Eq. (B8) in Appendix B.)

If $-\Phi_o = V_o$, where V_o is positive, the probe is accelerating and there may be trajectory exclusions manifested in θ_{max}. That is, θ_{max} may depend on V_o. However, in the absence of trajectory exclusions, θ_{max} is equal to $\pi/2$. In Appendix A it is shown that for a power-law potential falling off as r^{-n}, trajectory exclusions do not occur if n is less than 2. In this case, with $v_{\infty min} = 0$, the current is a linearly increasing function of V_o. According to Eq. (D19), this function may be expressed as:

$$\frac{I}{I_o} = 1 + \frac{2}{m} V_o \frac{\int_o^\infty \frac{dv}{v} N(v)}{\int_o^\infty v\, dv\, N(v)} \tag{D22}$$

where $N(v)$ is defined by Eq. (D20) and I_o is the value of I when $V_o = 0$. From this point on, the symbol v will be used to denote v_∞, since we will no longer refer to local velocities.

In the presence of trajectory exclusions due to intersections, θ_{max} depends on v and V_o. If we assume a power-law potential falling off as r^{-n} and use the results of the approximate theory in Appendix A,

we obtain the following expression for θ_{max}:

$$\sin^2\theta_{max} = \frac{2v^2 + \left(2 - \frac{n}{2}\right)\frac{2}{m}V_0}{v^2 + \frac{2}{m}V_0} \qquad \text{(power-law potential model)} \tag{D23}$$

for $v < v_1$, where v_1 is a critical velocity, defined by

$$v_1^2 = \left(\frac{n}{2} - 1\right)\frac{2}{m}V_0 \qquad \text{(power-law potential model)} \tag{D24}$$

For $v > v_1$, $\sin^2\theta_{max} = 1$. Equations (D23) and (D24) may be derived from Eqs. (A18) through (A21) of Appendix A, assuming that n has values lying between 2 and 4. Thus, the current may be written:

$$I = 2\pi r_0^2 \int_0^{v_1} \left[v^2 + \left(1 - \frac{n}{4}\right)\frac{2}{m}V_0\right] \frac{N(v)\,dv}{v}$$

$$+ \pi r_0^2 \int_{v_1}^{\infty} \left[v^2 + \frac{2}{m}V_0\right] \frac{N(v)\,dv}{v} \tag{D25}$$

The derivative of I with respect to V_o becomes:

$$\frac{dI}{dV_o} = \frac{2\pi r_o^2}{m}\left\{\left(2-\frac{n}{2}\right)\int_0^{v_1}\frac{N(v)\,dv}{v} + \int_{v_1}^{\infty}\frac{N(v)\,dv}{v}\right\} \qquad \text{(D26)}$$

As V_o becomes large, the slope becomes a positive constant proportional to (2 - n/2). (Compare with Eq. (C8) in Appendix C.) Thus, a saturation effect does not occur unless n exceeds 4.

The second derivative of I is given by

$$\frac{d^2I}{dV_o^2} = -\frac{\pi r_o^2}{mV_o}\left(\frac{n}{2}-1\right)N\left(\sqrt{\left(\frac{n}{2}-1\right)\frac{2}{m}V_o}\right) \qquad \text{(D27)}$$

which is equivalent to Eq. (C9) in Appendix C.

Thus, the current and its derivatives are given by precisely the same formulae as those given in Appendix C for the isotropic distribution, provided that the speed distribution is used in the formulae. This fact is due to the spherical symmetry of the probe potential. It may be shown that the theory applies to any speed distribution whatever, which is obtained from any velocity distribution by integration over all solid angles. The plausibility of this assertion may be seen as follows.

Equation (D19) may be derived alternatively by using the impact parameter picture, in which one considers the distribution of velocities at infinity to be composed of a number of beams of particles moving in parallel lines with equal velocities, as suggested in Reference 3 (p. 751). From the point of view of the particles in any of these beams, the potential distribution appears the same, due to its assumed spherical symmetry. Hence, the current entering the sphere depends only on the distribution of speeds of the particles, and one would obtain the correct answer by considering all the particles to be moving in a single parallel beam, but with the appropriate speed distribution function. Thus, a Maxwellian velocity distribution with superimposed drift has a speed distribution of the form

$$N(v) = 2\pi v^2 \int_0^{\pi} \frac{1}{\pi^{3/2}} e^{-v^2 - v_s^2 + 2 v v_s \cos\psi} \sin\psi \, d\psi$$

$$= \frac{1}{\sqrt{\pi}} \frac{v}{v_s} \left[e^{-(v - v_s)^2} - e^{-(v + v_s)^2} \right] \qquad \text{(D28)}$$

where the velocities are in units of $(2kT/m)^{\frac{1}{2}}$, v_s is the drift velocity Mach number, and the density is in units of n_o, the ambient particle density.

The current-voltage characteristics of a moving sphere have been calculated by Medicus[10] and Kanal[11], using the speed distribution Eq. (D28). Their calculations take the form of the potential into account by using the model of a sheath of definite thickness. The sheath thickness is the parameter which characterizes the form of the potential. According to the sheath model, $\sin^2\theta_{max}$ and v_i are defined by the following expressions:

$$\sin^2\theta_{max} = \frac{r_s^2}{r_0^2}\,\frac{v^2}{v^2 + \frac{2}{m}V_0} \qquad \text{(sheath model)} \qquad \text{(D29)}$$

$$v_1^2 = \frac{r_0^2}{r_s^2 - r_0^2}\,\frac{2}{m}V_0 \qquad \text{(sheath model)} \qquad \text{(D30)}$$

where r_s is the sheath radius. Equations (D29) and (D30) may be compared with Eqs. (D23) and (D24) based on the power-law potential model with n greater than 2.

COMPARISON OF MODELS

It will be of interest to compare the accelerating probe current-voltage characteristics derived on the basis of the power-law potential model with those derived on the basis of the sheath model, when $N(v)$ is given by Eq. (D28), corresponding to the physically interesting case of a Maxwellian with superimposed drift. In the power-law model the exponent n will be assumed to lie between 2 and 4.

For the power-law model, we will use Eqs. (D23) and (D24) in Eq. (D19). For the sheath model we will use Eqs. (D29) and (D30) in Eq. (D19). The current will be denoted by I_{PL} for the power-law model and by I_{SH} for the sheath model, and will be in units of $4\pi r_o^2 n_o (kT/2\pi m)^{\frac{1}{2}}$. With velocities in units of $(2kT/m)^{\frac{1}{2}}$ and potential energy in units of kT, the currents for both models may be expressed in the forms

$$I_{PL} = \alpha_{PL} I_o + \beta_{PL} F(v_{PL}) + \left(2 - \frac{n}{2}\right) V_o \frac{\sqrt{\pi}}{2v_s} \operatorname{erf} v_s \qquad \text{(D31)}$$

$$I_{SH} = \alpha_{SH} I_o + \beta_{SH} F(v_{SH}) \qquad \text{(D32)}$$

where

$$I_o = \frac{1}{2} e^{-v_s^2} + \left(\frac{1}{2} + v_s^2\right) \frac{\sqrt{\pi}}{2v_s} \operatorname{erf} v_s \qquad \text{(D33)}$$

and $F(v)$ is the function

$$F(v) \equiv \frac{v-v_s}{4v_s} e^{-(v+v_s)^2} - \frac{v+v_s}{4v_s} e^{-(v-v_s)^2}$$

$$+ \frac{1}{2v_s}\left[v^2 - v_s^2 - \frac{1}{2}\right]\frac{\sqrt{\pi}}{2}\left[\mathrm{erf}(v+v_s) - \mathrm{erf}(v-v_s)\right] \qquad \text{(D34)}$$

The arguments v_{PL} and v_{SH} are defined by

$$v_{PL} = \left(\frac{n}{2} - 1\right)^{1/2} V_0^{1/2} \qquad \text{(D35)}$$

and

$$v_{SH} = \gamma V_0^{1/2} \qquad \text{(D36)}$$

where

$$\gamma^2 \equiv \frac{r_0^2}{r_s^2 - r_0^2} \qquad \text{(D37)}$$

The coefficients α and β for the two models are defined by

$$\alpha_{PL} = 2 \qquad \beta_{PL} = 1 \tag{D38}$$

$$\alpha_{SH} = (1+\gamma^2)/\gamma^2 \qquad \beta_{SH} = 1/\gamma^2 \tag{D39}$$

When $V_o = 0$, both I_{PL} and I_{SH} become equal to I_o, defined by Eq. (D33). For small values of v_s, $F(v)$ approaches

$$F(v) \simeq -e^{-v^2}\left[1 + (2v^2+1)\frac{v_s^2}{3} + \cdots\right] \tag{D40}$$

For small values of v, $F(v)$ approaches

$$F(v) \simeq -I_o + \frac{v^2\sqrt{\pi}}{2v_s}\,\mathrm{erf}\, v_s + \cdots \tag{D41}$$

DIFFERENCES BETWEEN THE MODELS

For $v_s = 0$, I_{PL} and I_{SH} reduce to

$$(I_{PL})_{v_s=0} = 2 - e^{-V_0(\frac{n}{2}-1)} + (2-\tfrac{n}{2})V_0 \qquad \text{(D42)}$$

$$(I_{SH})_{v_s=0} = \frac{1+\gamma^2}{\gamma^2} - \frac{1}{\gamma^2}e^{-\gamma^2 V_0}$$

$$= \frac{r_s^2}{r_0^2} - \frac{(r_s^2 - r_0^2)}{r_0^2} e^{-\frac{r_0^2 V_0}{r_s^2 - r_0^2}} \qquad \text{(D43)}$$

Comparison of Eqs. (D42) and (D43) shows clearly that the sheath model current has a limiting ("saturation") current at large V_0, while the power-law model current does not, for n less than 4. This is the most important difference between the sheath and power-law models. When $v_s > 0$, and for large values of V_0, $F(v)$ approaches zero like $-e^{-v^2}$ in both models, and I_{PL} and I_{SH} become:

$$I_{PL} \sim 2I_0 + (2-\tfrac{n}{2})V_0 \frac{\sqrt{\pi}}{2v_s} \operatorname{erf} v_s \qquad (V_0 \to \infty) \qquad \text{(D44)}$$

$$I_{SH} \sim \frac{1+\gamma^2}{\gamma^2} I_0 \qquad (V_0 \to \infty) \qquad \text{(D45)}$$

That is, the saturation effect is exhibited by I_{SH}, but not by I_{PL}, when n is less than 4.

For small values of v_s, $F(v)$ is given by Eq. (D40), I_o approaches $1 + v_s^2/3$, $(\sqrt{\pi}/2v_s)\,erf\, v_s$ approaches $1 - v_s^2/3$, and I_{PL} and I_{SH} approach:

$$I_{PL} \simeq (I_{PL})_{v_s=0} + \frac{v_s^2}{3}\left[(I_{PL})_{v_s=0} - (n-2)V_o e^{-\left(\frac{n}{2}-1\right)V_o} + (n-4)V_o\right] \quad (D46)$$

$(v_s << 1)$

$$I_{SH} \simeq (I_{SH})_{v_s=0} + \frac{v_s^2}{3}\left[(I_{SH})_{v_s=0} - 2V_o e^{-\gamma^2 V_o}\right] \quad (D47)$$

$(v_s << 1)$

Hence, the forms of I_{PL} and I_{SH} differ in that I_{PL} has an additional linear term. Thus, for large values of V_o, and small values of v_s, I_{PL} and I_{SH} approach

$$I_{PL} \sim 2\left(1 + \frac{1}{3}v_s^2\right) + \left(2 - \frac{n}{2}\right)V_o\left(1 - \frac{1}{3}v_s^2\right) \quad (D48)$$

$(V_o >> 1,\ v_s << 1)$

$$I_{SH} \sim \frac{1+\gamma^2}{\gamma^2}\left(1 + \frac{1}{3}v_s^2\right) \quad (D49)$$

$(V_o >> 1,\ v_s << 1)$

SIMILARITIES BETWEEN THE MODELS

For small values of v, $F(v)$ is given by Eq. (D41). Thus, for small values of V_o, I_{PL} and I_{SH} become equal and are given by

$$I_{PL} = I_{SH} \simeq I_o + V_o \frac{\sqrt{\pi}}{2v_s} \operatorname{erf} v_s \qquad (V_o \ll 1) \quad \text{(or } n=2, \text{ or } \gamma=0) \qquad \text{(D50)}$$

where I_o is defined by Eq. (D33).

For n = 2, $F(v_{PL})$ becomes equal to $-I_o$, and I_{PL} is given by Eq. (D50). For $\gamma \to 0$, which corresponds to an infinitely thick sheath,

$$\beta_{SH} F(v_{SH}) \to -\frac{I_o}{\gamma^2} + V_o \frac{\sqrt{\pi}}{2v_s} \operatorname{erf} v_s \qquad \text{(D51)}$$

Hence, from Eq. (D32) we obtain for I_{SH} the expression given in Eq. (D50). Thus, for n = 2 (or less) we obtain the same current, based on the power-law model, as we obtain for the sheath model with $\gamma = 0$. That is, the two models become equivalent in this limit. In other words, the infinite sheath case corresponds to the case of no trajectory exclusions due to intersections, which we have shown, in Appendix A, to be valid when the potential falls off like r^{-n} and n is less than 2.

Moreover, I_{PL} for n= 4 becomes identical to I_{SH} for $\gamma = 1$. For these values,

$$v_{PL} = v_{SH} = V_o^{1/2} \qquad \text{(D52)}$$

and the currents become

$$\left(I_{PL}\right)_{n=4} = \left(I_{SH}\right)_{\gamma=1} = 2I_o + F\left(V_o^{1/2}\right) \qquad \text{(D53)}$$

Thus, in this case, I_{PL} shows saturation for large V_o as well as I_{SH}. Now Eq. (D31) for I_{PL} is invalid for $n > 4$, but, according to the discussion of Appendix A the current I_{PL} probably will saturate at large V_o when n exceeds 4. Hence, for n greater than 4, the two models are probably equivalent also. In the limit of infinite n, I_{PL} should become equal to I_o, as does I_{SH} in the limit of infinite γ (thin sheath limit).

Finally, the sheath thickness should be an increasing function of V_o.[5] Therefore, the "saturation" effect exhibited by I_{SH} at large V_o, i.e. Eq. (D45), is only an apparent effect. Therefore, for large sheath thicknesses, i.e. where γ is less than unity, the power-law model ($n < 4$) probably affords a better description of the current characteristics. Whereas, for small sheath thicknesses, where γ is greater than unity, the sheath model may have greater validity.

The current I_{PL} is plotted for $v_s = 0$, 1, and 2 in Figs. D2, D3 and D4, respectively. In each figure, curves are plotted for n = 2, 3 and 4.

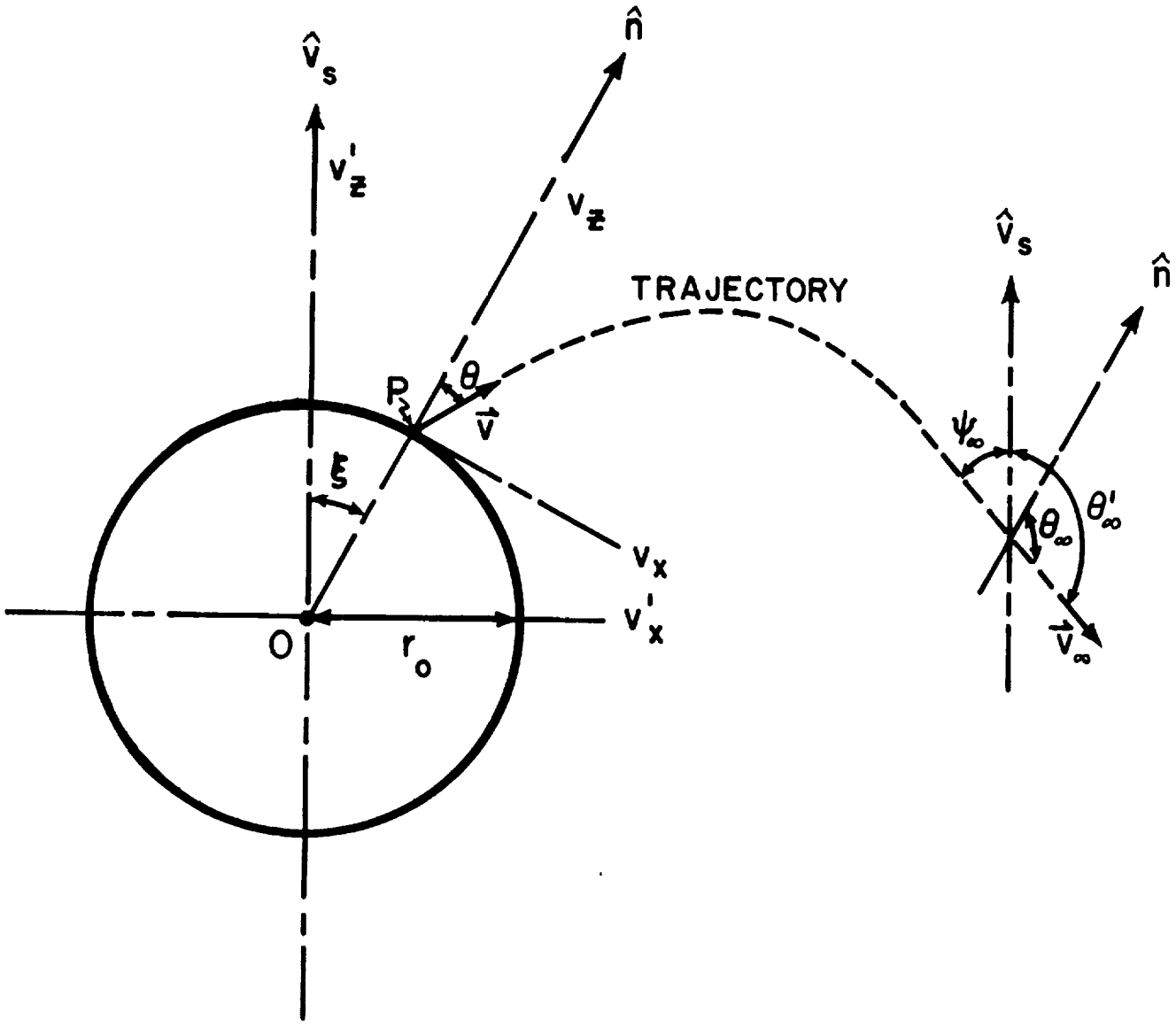

FIGURE D1. ROTATION OF COORDINATE SYSTEM FOR SURFACE INTEGRATION

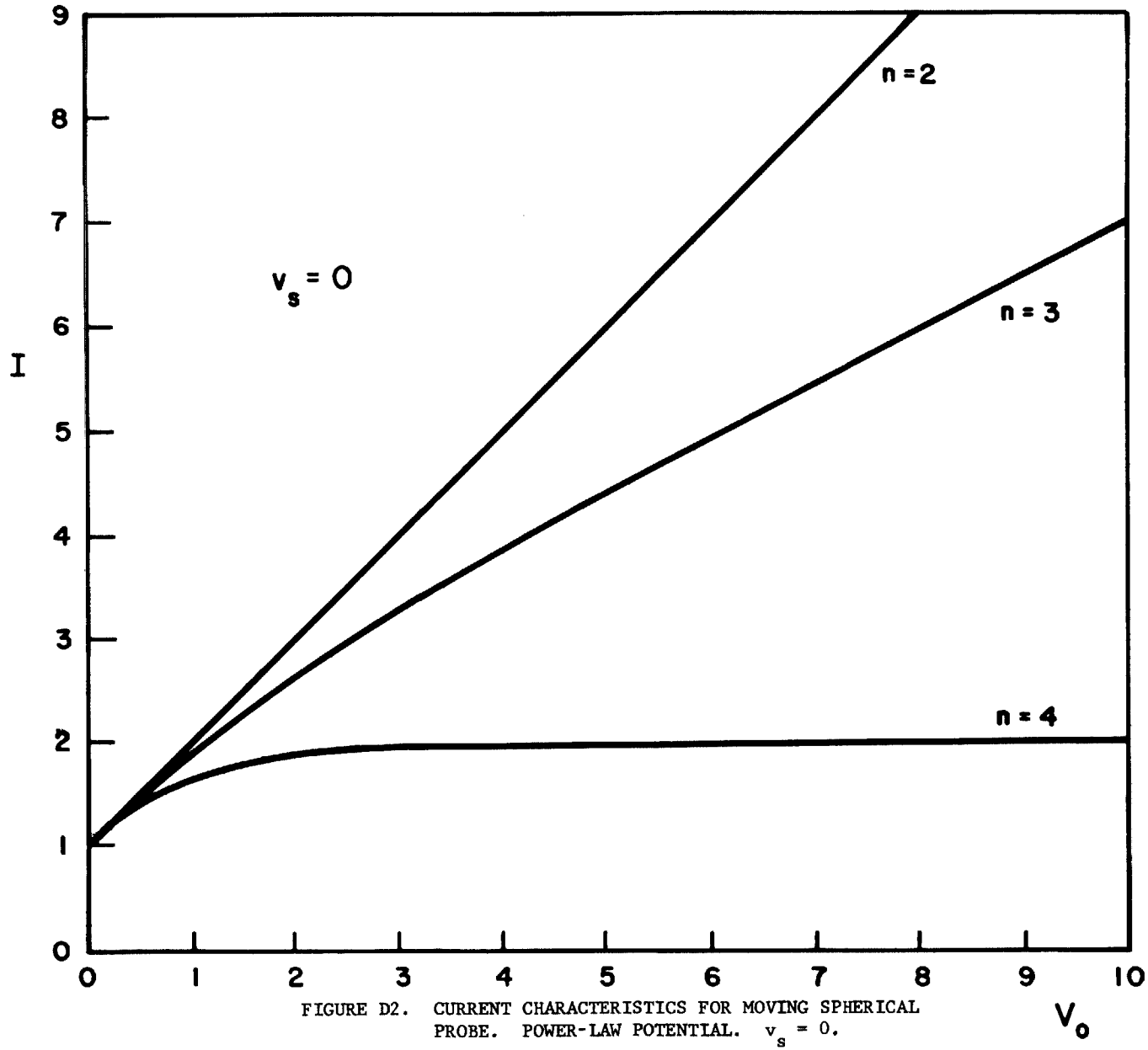

FIGURE D2. CURRENT CHARACTERISTICS FOR MOVING SPHERICAL PROBE. POWER-LAW POTENTIAL. $v_s = 0$.

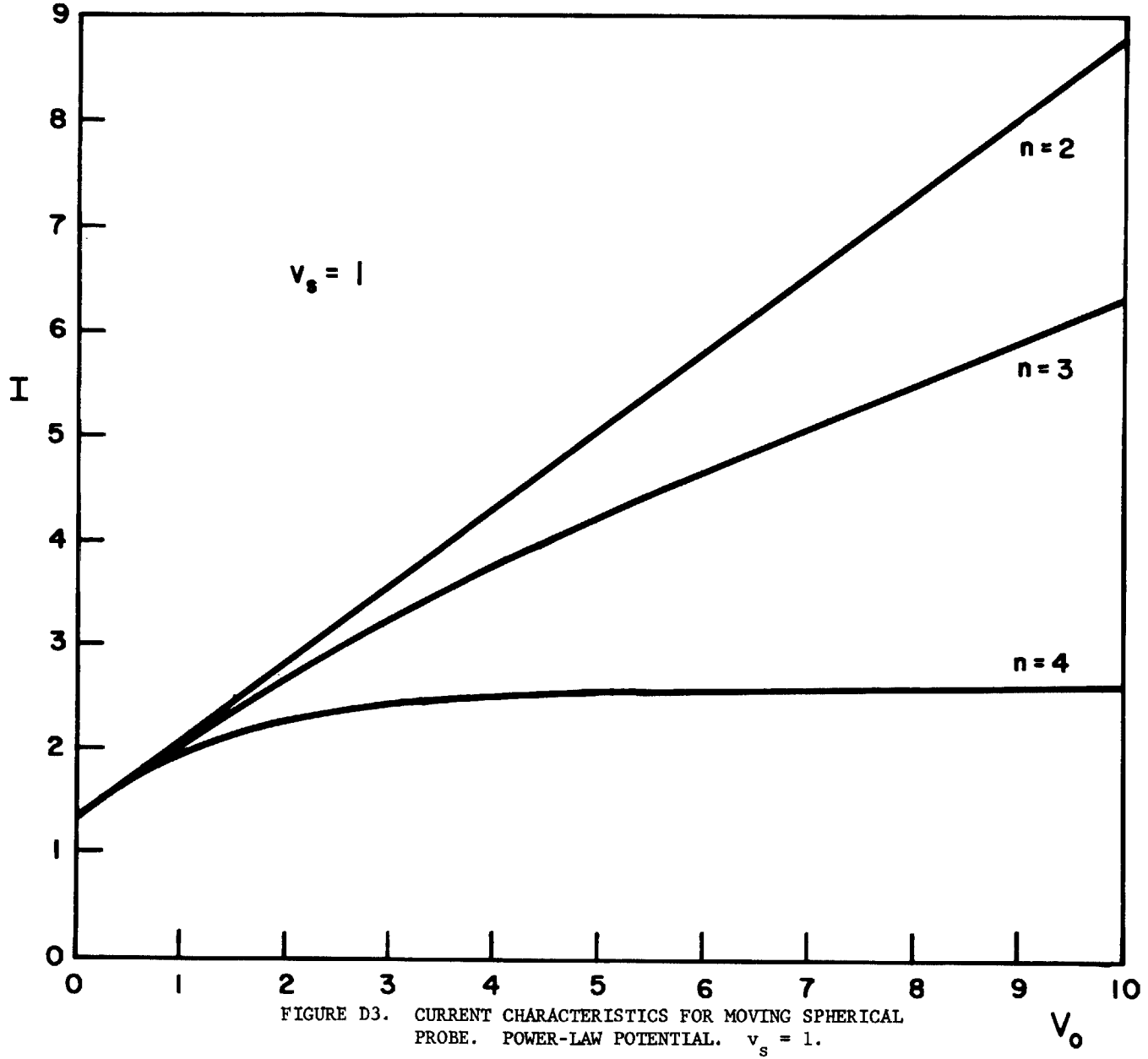

FIGURE D3. CURRENT CHARACTERISTICS FOR MOVING SPHERICAL PROBE. POWER-LAW POTENTIAL. $v_s = 1$.

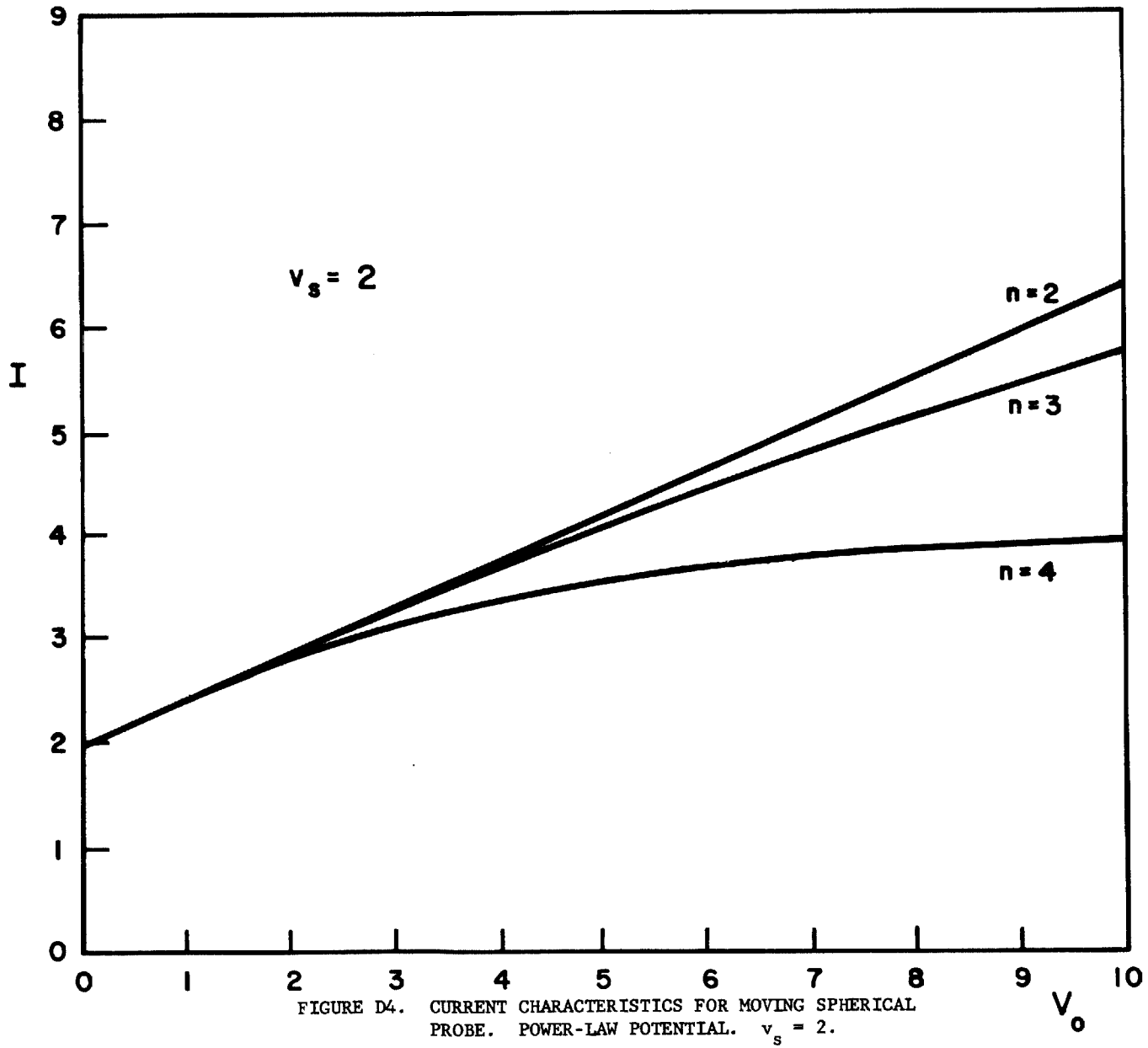

FIGURE D4. CURRENT CHARACTERISTICS FOR MOVING SPHERICAL PROBE. POWER-LAW POTENTIAL. $v_s = 2$.

REFERENCES

1. See, for example, R. E. Bourdeau, J. L. Donley, G. P. Serbu, and E. C. Whipple, Jr., "Measurements of sheath currents and equilibrium potential on the Explorer VIII satellite," National Aeronautics and Space Administration Report TND-1064 (Greenbelt Space Flight Center), July 1961. See also R. E. Bourdeau and J. L. Donley, "Explorer VIII satellite measurements in the upper ionosphere," Proc. Roy. Soc. A 281, 487-504 (1964).

2. M. J. Druyvesteyn, "Der neidervoltbogen," Z. Physik 64, 781-798 (1930).

3. H. M. Mott-Smith and I. Langmuir, "Theory of collectors in gaseous discharges," Phys. Rev. 28, 727-763 (1926).

4. L. S. Hall, "Probes and magnetic pumping in plasma," University of California Lawrence Radiation Laboratory Report UCRL-6535, July 1961.

5. I. B. Bernstein and I. N. Rabinowitz, "Theory of electrostatic probes in a low-density plasma," Phys. Fluids 2, 112-121 (1959).

6. Ya. L. Al'pert, A. V. Gurevich and L. P. Pitaevskii, Space Physics with Artificial Satellites, Consultants Bureau, New York, 1965.

7. L. W. Parker, "A computer program for calculating the charge distribution about a space vehicle," American Astronautical Society Second Symposium on Interaction of Space Vehicles with an Ionized Atmosphere, Miami Beach, November 1965. (NASA CR-401, March 1966).

8. The Orbiting Geophysical Observatory planar ion and electron trap, designed by E. C. Whipple, Jr. (private communication).

9. The boundary of the allowed domain of integration is considered for the spherically symmetric problem in References 4, 5, and 6. The domain is formulated in terms of a velocity space in Reference 6, and in terms of an energy-angular momentum space in References 4 and 5.

10. G. Medicus, "Theory of electron collection of spherical probes," J. Appl. Phys. 32, 2512-20 (1961); "Spherical Langmuir probe in 'drifting' and 'accelerated' Maxwellian distribution," J. Appl. Phys. 33, 3094-3100 (1962).

11. M. Kanal, "Theory of current collection of moving spherical probes," University of Michigan Space Research Laboratory Report No. JS-5, April, 1962.

12. F. Smetana, "On the current collected by a charged circular cylinder immersed in a two-dimensional rarefied plasma stream," Third Symposium on Rarefied Gas Dynamics, Vol. II, Ed. J. A. Laurmann, Academic Press, 1963.

NASA-Langley, 1967 CR-704